# Morphology-dependent Photophysical Properties of Poly-4-vinylpyridine Polymers Containing –Re(CO)$_3$(N^N)$^+$ Pendants

## Ezequiel Wolcan

*Instituto de Investigaciones Fisicoquímicas Teóricas y Aplicadas (INIFTA, UNLP, CCT La Plata--CONICET), Argentina.*
*Email: ewolcan@inifta.unlp.edu.ar*

**Abstract**

We review the morphological and the photophysical properties of several inorganic polymers that can be prepared from poly-4-vinylpyridine (P4VP). These polymers contain –Re(CO)$_3$(N^N)$^+$ pendants attached to their backbone with α-diimine ligands (N^N) such as 2,2´-bipyridine (bpy), 1,10-phenanthroline (phen), 3,4,7,8-tetramethyl-1,10-phenanthroline (tmphen) and 5-nitro-1,10-phenanthroline (NO$_2$-phen). These Re(I) polymers, show marked differences in their photophysical properties when compared to single [pyRe(CO)$_3$(N^N)]$^+$ molecules in diluted solutions. For example, Re→phen charge transfer excited states (MLCT) in the Re(I) polymers undergo a more efficient annihilation and/or secondary photolysis than in [pyRe(CO)$_3$phen]$^+$ complexes. Depending on solvent and/or cast film conditions, several aggregates of polymer strands with different morphologies were observed by transmission electron microscopy (TEM) and dynamic light scattering (DLS) techniques. Morphological changes derived from media-imposed changes (solvent, temperature) or from polymer backbone chemical modifications (protonation or peralkylation in P4VP uncoordinated pyridines) are responsible for the marked differences observed between the photophysical properties of these Re(I) polymers and those of the single pyRe(CO)$_3$(N^N)$^+$ molecules. Therefore, these Re(I) polymers can provide a good reaction scenario for other photochemical reactions. Thus, resonance energy transfer between –Re(CO)$_3$(tmphen)$^+$ and –Re(CO)$_3$ (NO$_2$-phen)$^+$ pendants was observed in Re(I)-P4VP polymers containing both chromophores attached to their backbone. In addition, in the quenching of the MLCT luminescence of –Re(CO)$_3$(N^N)$^+$ pendants by amines, we observed a retardation of the molecular motion due to the restricted media that favored the observation of the Marcus *inverted effect* in bimolecular reactions due to the fact that low values of the solvent reorganization energies are achieved within aggregates.
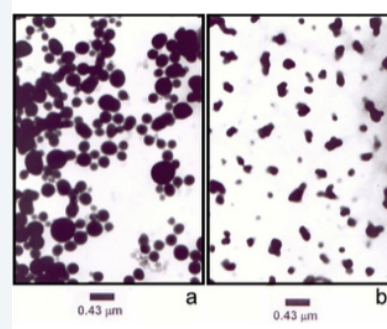
**Keywords**:
poly-4-vinylpyridine polymers, –Re(CO)3(N^N)+ pendants, Marcus inverted effect

## Introduction

From the third row of transition metal compounds, Re(I) complexes have been of considerable research interest during the last four decades. In particular, Re(I)(CO)$_3$ complexes coordinating mono or bidentate azines of the type *fac-*

LRe(CO)$_3$(N^N) (where L= halide and/or substituted azine and N^N = α-diimine, Scheme 1) show exceptionally rich excited-state behavior and redox chemistry as well as thermal and photochemical stability.[1] Through broad structural variations of the N^N ligand, they can be used in electron transfer studies,[2] solar energy conversion[3-5] and catalysis,[6] as luminescent sensors,[7-9] molecular materials for non-linear optics[10,11] and optical switching.[12] Additionally, the variation of L/N^N ligands allows incorporating these chromophores into several media such as proteins,[13-15] intercalating them into DNA,[16,17] or making them part of supramolecular structures.[18]
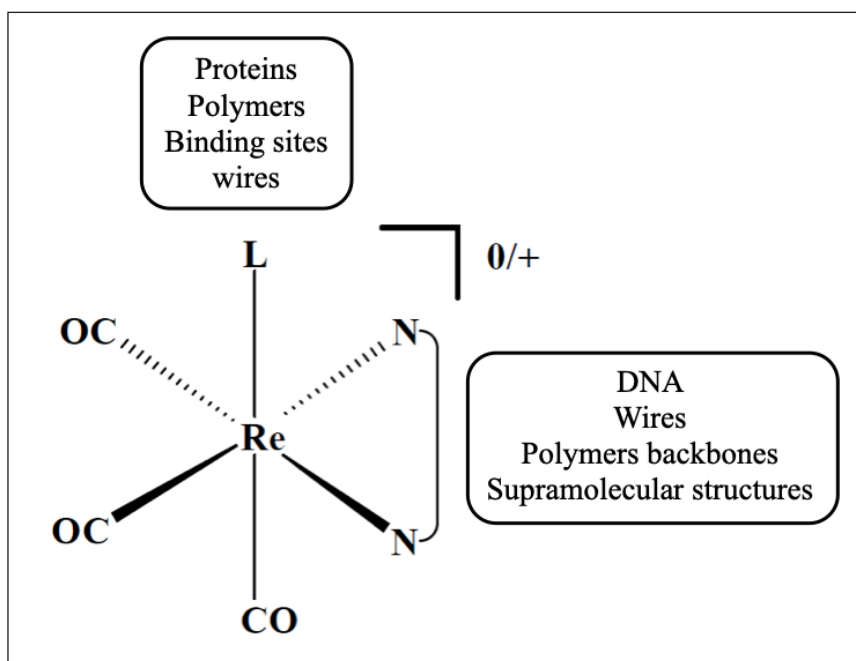


**Scheme 1.** Structural formulae of *fac*-LRe(CO)$_3$(N^N) complexes. The complexes are neutral or positively charged for anionic or neutral axial ligands, L, respectively. Broad variations of L and/or equatorial (N^N) ligands allows to incorporate those complexes into several media, such as proteins, DNA, binding sites, wires, polymers and supramolecular structures.

Heterogeneous media such as micelles, organic polymers and microporous materials can provide a good reaction scenario for photochemical reactions. In addition, inorganic polymers present unique properties compared to those of their organic analogues. For instance, with the incorporation of inorganic elements within a polymeric backbone, a rich variety of different coordination numbers and geometries which are inaccessible with carbon-based organic backbones also become available. Moreover, the introduction of metallic elements offers the possibility of redox or catalytic activity and ready access to stable structures that possess unpaired electrons.

When transition metal compounds are attached to organic polymeric backbones, the metallic complexes can be confined within small spaces, and distances as low as 8Å may be encountered between two metallic centers, giving rise to new photochemical pathways that are not observed in diluted solutions of the simple molecules;[19] see Scheme 2. These small distances between metallic centers can be compared to the mean distances encountered in liquid solutions; eq. 1

$$R \text{ (in } Å) = \frac{6.5}{\sqrt[3]{C}} \tag{1}$$

where C is the concentration in M units. Using a typical value for $C$ in a photochemical experiment (i.e. $C \sim 1\text{x}10^{-4}$ M), a value of $R \sim 140$ Å is obtained. It is only at concentrations $C > 0.5$ M that mean distances between metal centers reach values of around 8 Å.
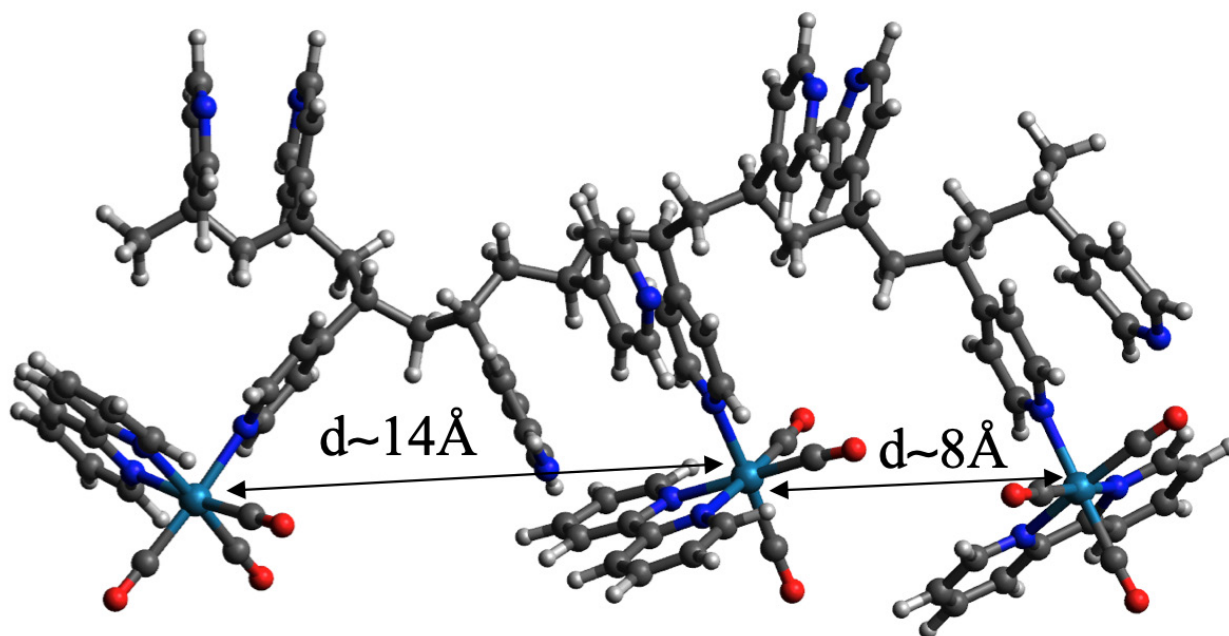
**Scheme 2.** Representation of a fragment (only three Re(I) chromophores are represented here) of polymer $[(vpy)_2\text{-}vpyRe(CO)_3(bpy)]_{n\sim200}(CF_3SO_3)_{n\sim200}$ showing mean inter-chromophore distances.

Polymers containing transition metal chromophores have been prepared where group phenomena such as fast, site-to-site energy transfer hopping and photochemically induced electron transfer have been observed.[20] Much of the literature examples involve transition metal ions metalating poly(p-phenylenevinylene) polymers incorporating 2,2-bipyridines,[21-23] polypyridil Ru(II) and/or Os(II) derivatized polystyrene[20,24-33] and some multimetallic oligomeric complexes containing Ru(II) and Os(II) coordinated to 1,10-phenanthroline (phen).[34] However, little attention was paid to Re(I) polymeric complexes, and only a few examples can be found in the literature up to the beginning of the new century.[35] After 2000, however, there has been a huge development in the field, mainly due to our research,[19,36-46] and the work of the research group led by Chan.[47,48]

## 1. Poly-4-vinylpyridine as a successful scaffold for new photochemical/morphology dependent phenomena

The polymers used in our works have been derived from the poly-4-vinylpyridine (P4VP) backbone and they contain $-Re(CO)_3(N^\wedge N)^+$ pendants in their structure. P4VP has a molecular weight of $M_w \sim 6,0\times10^4$ and, on average, it contains about 600 vinylpyridine (vpy) units per formula. These inorganic polymers are synthesized by attaching pendant chromophores $-Re(CO)_3(N^\wedge N)^+$ to one third of the pyridines of the organic backbone (Scheme 3). The polymers can be assigned the formal structure of Scheme 3 where pendant $-Re(CO)_3(N^\wedge N)^+$ groups are randomly distributed along the strand of polymer with an average of two uncoordinated 4-vinylpyridine groups for each one coordinated to a Re(I) chromophore. The molecular weights of the final polymers range from 1.7 to $2.0\times10^5$ depending on the nature of the ligand $(N^\wedge N)$ used in polymer synthesis (Scheme 3).
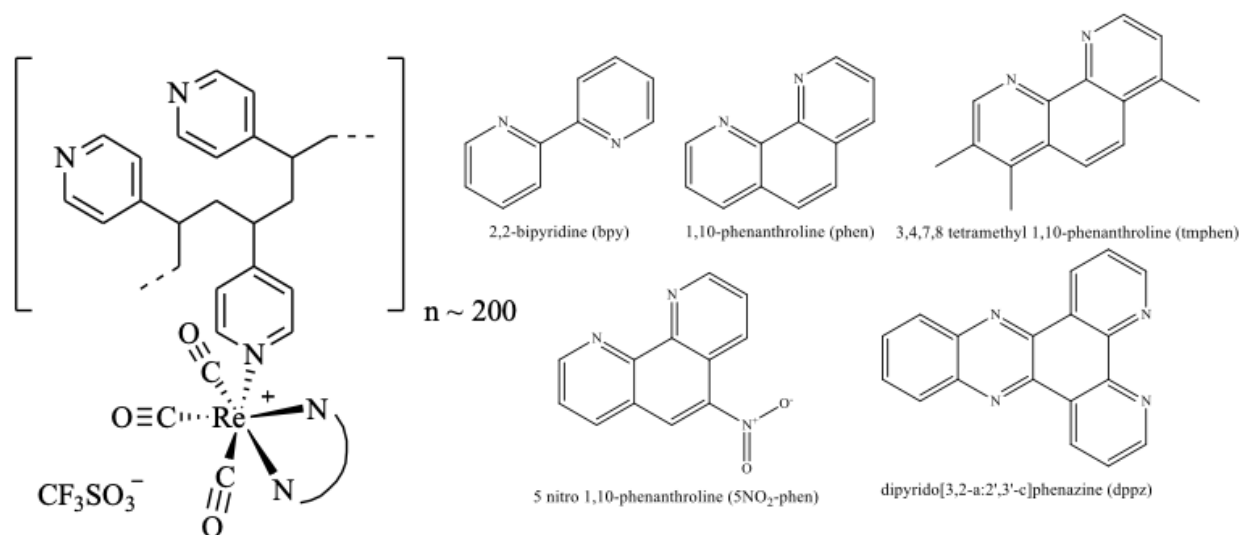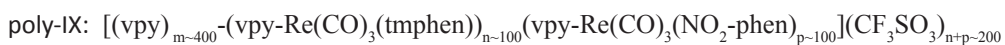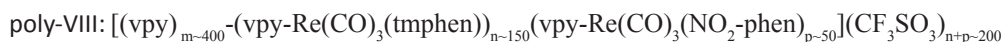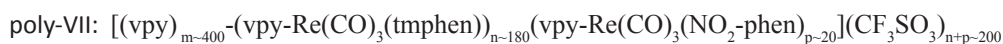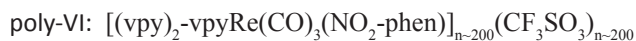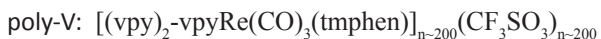
**Scheme 3.** Structural formulae of polymers derived from poly-4-(vinylpyridine) and –Re(CO)$_3$(N^N)$^+$ pendants with selected α-diimine ligands and the abbreviations used (in parenthesis).

The polymers were obtained in good yields (>80 %) by direct reaction of their respective Re(CO)$_3$(N^N)CF$_3$SO$_3$ complexes with P4VP in dichloromethane reflux under a N$_2$ blanket according to eq. 2

$$200 \, Re(CO)_3(N^\wedge N)CF_3SO_3 + P4VP \rightarrow [(vpy)_2\text{-}vpyRe(CO)_3L]_{n\sim200}(CF_3SO_3)_{n\sim200} \qquad (2)$$

Thus, the following polymers were obtained:

poly-I: $[(vpy)_2\text{-}vpyRe(CO)_3(phen)]_{n\sim200}(CF_3SO_3)_{n\sim200}$

poly-II: $[(vpy)_2\text{-}vpyRe(CO)_3(bpy)]_{n\sim200}(CF_3SO_3)_{n\sim200}$

poly-III: $[(vpy)_{m\sim338}\text{-}(vpy\text{-}Re(CO)_3(bpy))_{n\sim131}(vpy\text{-}Re(CO)_3(phen)_{p\sim131}](CF_3SO_3)_{n+p\sim262}$

poly-IV: $[(vpy)_{m\sim250}\text{-}(vpy\text{-}Re(CO)_3(bpy))_{n\sim200}(vpy\text{-}Re(CO)_3(phen)_{p\sim150}](CF_3SO_3)_{n+p\sim350}$

poly-V: $[(vpy)_2\text{-}vpyRe(CO)_3(tmphen)]_{n\sim200}(CF_3SO_3)_{n\sim200}$

poly-VI: $[(vpy)_2\text{-}vpyRe(CO)_3(NO_2\text{-}phen)]_{n\sim200}(CF_3SO_3)_{n\sim200}$

poly-VII: $[(vpy)_{m\sim400}\text{-}(vpy\text{-}Re(CO)_3(tmphen))_{n\sim180}(vpy\text{-}Re(CO)_3(NO_2\text{-}phen)_{p\sim20}](CF_3SO_3)_{n+p\sim200}$

poly-VIII: $[(vpy)_{m\sim400}\text{-}(vpy\text{-}Re(CO)_3(tmphen))_{n\sim150}(vpy\text{-}Re(CO)_3(NO_2\text{-}phen)_{p\sim50}](CF_3SO_3)_{n+p\sim200}$

poly-IX: $[(vpy)_{m\sim400}\text{-}(vpy\text{-}Re(CO)_3(tmphen))_{n\sim100}(vpy\text{-}Re(CO)_3(NO_2\text{-}phen)_{p\sim100}](CF_3SO_3)_{n+p\sim200}$

poly-X: $[(vpy\text{-}CH_3^+)_2\text{-}vpyRe(CO)_3(phen)]_{n\sim200}(CF_3SO_3)_{n\sim600}$

poly-XI: $[(vpy)_2\text{-}vpyRe(CO)_3(dppz)]_{n\sim200}(CF_3SO_3)_{n\sim20}$

where poly-X, i.e. $[(vpy\text{-}CH_3^+)_2\text{-}vpyRe(CO)_3(phen)]_{n\sim200}(CF_3SO_3)_{n\sim600}$ was obtained by peralkylation of the free pyridines of poly-I; eqs. 3-4

$$[(vpy)_2\text{-}vpyRe(CO)_3(phen)]_{n\sim200}(CF_3SO_3)_{n\sim200} \xrightarrow{\text{ICH}_3}$$

$$[(vpy\text{-}CH_3^+)_2\text{-}vpyRe(CO)_3(phen)]_{n\sim200}(CF_3SO_3)_{n\sim200}(I)_{m\sim400} \qquad (3)$$

$$[(vpy\text{-}CH_3^+)_2\text{-}vpyRe(CO)_3(phen)]_{n\sim200}(CF_3SO_3)_{n\sim200}(I)_{m\sim400} \xrightarrow[-\text{AgI}]{\text{AgCF}_3\text{SO}_3}$$

$$[(vpy\text{-}CH_3^+)_2\text{-}vpyRe(CO)_3(phen)]_{n\sim200}(CF_3SO_3)_{n\sim600} \qquad (4)$$
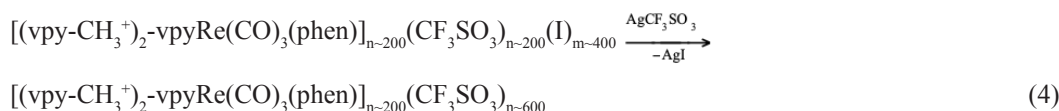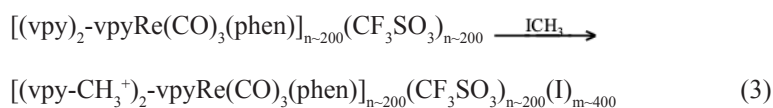
These polymers display interesting as well as intriguing features both in photochemistry and in material science, which we will discuss in the following sections. From a historic perspective, however, it should be noted that when we started our research with poly-I,[42] poly-II[40] and poly-X,[44] we were unaware of their morphology and the fact that morphological changes could affect the photochemical properties of these polymers. This initial *unawareness* was mainly because in previous studies that appeared in the literature, i.e. those Ru(II) and Os(II) polymers[20-34] previously mentioned in the introduction, there was a lack of morphological studies. It was not up until the work carried out by Chan's group,[47,48] and almost in parallel by our work,[39] that the morphological properties of those inorganic polymers were taken into account and studied in depth.

## 2. Contrasting the photophysical properties of poly-I and poly-X with those of [pyRe(CO)₃phen]⁺ complex

The UV-vis spectra of poly-I and $pyRe(CO)_3phen^+$ exhibited similar features. The extinction coefficients of poly-I, however, by comparison to the extinction coefficients of the molecular complex, corresponded to ~200 chromophores, $-Re(CO)_3phen^+$, per formula weight of polymer. This was in good agreement with the load of Re(I) pendants expected from the calculation from the elemental analysis and with the structures shown in Scheme 3.

Identical band shapes from the emission spectra were observed in $N_2$-degassed $CH_3CN$ solutions of $[pyRe(CO)_3phen]^+$ and poly-I centered at $\lambda_{max} = 560$ and 565 nm, respectively. Flash photolysis experiments irradiating with $\lambda_{exc} = 351$ nm to either poly-I or $[pyRe(CO)_3phen]^+$ complex in deaerated $CH_3CN$ produced nearly identical transient absorption spectra, respectively, assigned to the $^3$MLCT excited states. The $^3$MLCT excited state spectra, $\lambda_{max} \sim 460$ nm and $\lambda_{max} \sim 750$ nm, remained the same and did not change with the number $n_{hv}$ of 351 nm photons absorbed by either $[pyRe(CO)_3phen]^+$ or by the $-Re(CO)_3phen^+$ pendant chromophores of poly-II.[42] Conversely, the quantum yield of the MLCT excited state, $\Phi_{MLCT}$, and its lifetime, showed marked dependences on $n_{hv}$ and the photogenerated MLCT excited state concentration. For $[pyRe(CO)_3phen]^+$, despite the fact that $\Phi_{MLCT}$ was nearly independent of $n_{hv}$ for $n_{hv}$ values that were below 20% of the total Re(I) concentration, it decreased monotonically above that limit. Similar experiments carried out with solutions of poly-I in $CH_3CN$ or $MeOH/H_2O$ mixed solvent showed that $\Phi_{MLCT}$ decreased with $n_{hv}$ and reached the same value of that of $[pyRe(CO)_3phen]^+$ in the limit $n_{hv} \rightarrow 0$ (see Figure 1). In addition, the disappearance of the MLCT excited states in $[pyRe(CO)_3phen]^+$ and in the Re(I) polymer occurred with different reaction kinetics. The decay of the $^3$MLCT excited states of the pendant chromophores of poly-I exhibited more marked second order behavior than the decay of the $^3$MLCT excited states of $[pyRe(CO)_3phen]^+$. As shown in Figure 2, the linear dependence of $t_{1/2}$ on the reciprocal of the MLCT concentration demonstrated that the MLCT decay was kinetically of a second order on the MLCT concentration for $n_{hv}$ values larger than 17% of the total Re(I) concentration. A similar study of the MLCT decay kinetics with $[pyRe(CO)_3phen]^+$ established that traces were well fitted to a single exponential and the lifetime exhibited no dependence on MLCT concentration until $n_{hv}$ corresponded to 30% of the Re(I) concentration. These experimental observations showed that the process whose rate was kinetically of a second order in MLCT concentration contributed less to the excited state decay in $[pyRe(CO)_3phen]^+$.[42]

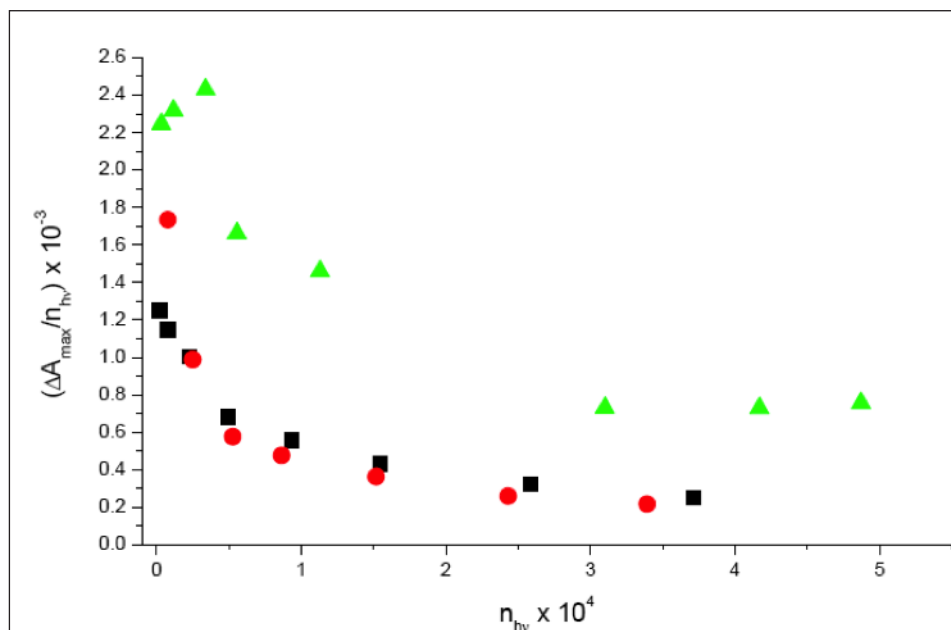**Figure 1.** Dependence of the MLCT excited-state quantum yield, $\varphi_{MLCT}$ (assumed proportional to $\Delta A_{max}/n_{hv}$), on $n_{hv}$ in laser flash photolysis (351 nm) of [pyRe(CO)$_3$phen]$^+$ and Poly-I. Solutions of the Re(I) complexes in deaereated CH$_3$CN were used with [pyRe(CO)$_3$phen]$^+$ (▲) and Poly-I (■). Solutions in deaereated MeOH/H$_2$O (1:4) of the Re(I) polymer were used in (●) experiments. Reprinted with permission from ref. 42. Copyright 2005 American Chemical Society.
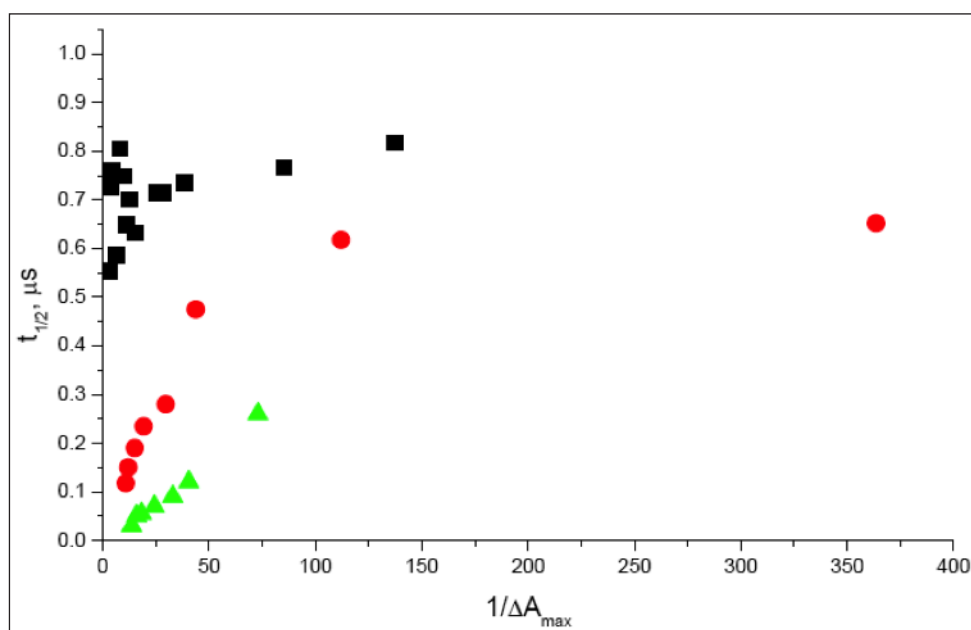


**Figure 2.** Dependence of MLCT state $t_{1/2}$ on $1/\Delta A_{max}$ for [pyRe(CO)$_3$phen]$^+$ in CH$_3$CN (■), for Poly-I in CH$_3$CN (●) and for Poly-I in MeOH-H$_2$O (▲). Reprinted with permission from ref. 42. Copyright 2005 American Chemical Society.

From a photochemistry standpoint, these Re(I) polymers, show marked differences in their photophysical properties when compared to single [pyRe(CO)$_3$phen]$^+$ molecules in diluted solutions. For example, Re→phen charge transfer excited states (MLCT) in the Re(I) polymers undergo a more efficient annihilation and/or secondary photolysis than in [pyRe(CO)$_3$phen]$^+$ complexes; eq. 5-6.[42]

$$[-Re(CO)_3phen]^+ \xrightleftharpoons[hv_{em}]{hv} {}^3MLCT \xrightarrow{hv} [-Re(CO)_3phen]^{+*} \qquad (5)$$

$$2\,({}^3MLCT) \xrightarrow{\phantom{xxx}} [-Re(CO)_3phen]^+ + [-Re(CO)_3phen]^{+*} \qquad (6)$$
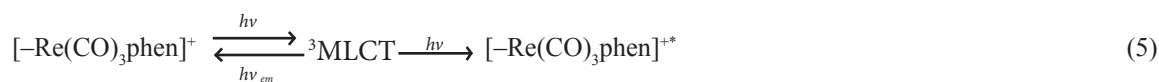
In these equations, $[-Re(CO)_3Lphen]^{+*}$ denotes an excited state higher in energy than the MLCT assigned as an intra-ligand, IL, excited state, generated in the $-Re(CO)_3phen^+$ pendant chromophore. In Equation 5, the annihilation of two $^3$MLCT excited states forms chromophores in the ground state and intra-ligand, IL, excited states. In contrast to the $^3$MLCT, the $^3$IL excited states oxidize solvents like $CH_3OH$.[42]

Absorption of light by MLCT excited states in the polymer to form intraligand excited states, IL, accounts for the functional dependence of $\Phi_{MLCT}$ on $n_{hv}$ explaining a decrease of $\Phi_{MLCT}$ with $n_{hv}$ at lower $n_{hv}$ values than the decrease of $\Phi_{MLCT}$ with $n_{hv}$ observed with $[pyRe(CO)_3phen]^+$ molecules. Because the IL excited state is shorter-lived than the MLCT excited state, the decay represented in Equation 5 is faster than the instrument's 20 ns response, and it was manifested only by a smaller photogenerated concentration of MLCT in the polymer than the expected one. A fast intrastrand annihilation of MLCT excited states also provides a good rationale for the functional dependence of $\Phi_{MLCT}$ on $n_{hv}$. In this mechanism, the rapid curvature of $\Phi_{MLCT}$ with $n_{hv}$ in Figure 1 requires that a large fraction of photogenerated excited states vanishes within the 20 ns laser pulse. Within the strand of polymer, if excited Re chromophores are close neighbors and have the right spatial orientation, they may undergo a fast annihilation within that period of time. This fast annihilation process can create IL excited states that are placed at higher energies and that are more reactive than the parent MLCT excited state.

The excited chromophores that have not experienced a fast annihilation or secondary photolysis due to being disfavored by reason of their position will be observed at times longer than the 20 ns laser irradiation. Flash photolysis shows that the rate of decay of this remnant excited state population is kinetically of a second order in the overall MLCT concentration. The second-order kinetics indicates that mechanisms by which the energy moves through the strand of polymer are available, since diffusive motions of the polyelectrolyte are much slower than those of the observed decay of excited states. Various mechanisms of intramolecular energy transfer have been proposed for organic polymers.[42] For instance, energy hopping in the strand may form pairs of excited chromophores that undergo annihilations. Experimental observations with poly-X, in which uncomplexed pendant pyridine groups of poly-I are methylated, support this mechanism, as quaternization of the pyridine groups to form poly-X enhanced electron transfer through the strand of the polymer.[44] The process could involve excited states of the uncomplexed pyridine pendants. It is also possible that energy can be transferred between remotely placed excited chromophores. These events will leave, therefore, one chromophore in the ground state and the other in an upper intraligand excited state, IL. This process is in contrast with the intrastrand energy transfers that occur during the irradiation of a P4VP polymer containing pendants $-[Re(CO)_3(phen)]^+$ chromophores.[42]

## 3. Laser power, thermal and solvent effects on the photophysical properties of poly-II

The emission spectra of $[pyRe(CO)_3bpy]^+$ and that of poly-II showed a distinctive behavior in solvent mixtures. In deoxygenated DMSO-$CH_3CN$ (1 : 9 v/v) mixtures at room temperature, the emission spectra of $[pyRe(CO)_3bpy]^+$ and poly-II exhibited unstructured bands with similar band shapes centered at 575 and 577 nm, respectively. For both poly-II and $[pyRe(CO)_3bpy]^+$, the emission maximum shifted to 569 nm in DMSO-$CH_2Cl_2$ (1 : 9 v/v). In DMSO-water (1 : 9 v/v) mixtures, however, the emission maximum for $[pyRe(CO)_3bpy]^+$ was observed at 574 nm, while in the case of poly-II, it shifted to $\lambda_{max}$ = 561 nm.[40]

Emission decays in the mixed solvents DMSO-$CH_3CN$, DMSO-$CH_2Cl_2$ and DMSO–water were monoexponential for $CF_3SO_3[pyRe(CO)_3bpy]$. However, for poly-II, monoexponential emission decays were only observed with DMSO-$CH_3CN$ mixtures, while in DMSO–water and DMSO–$CH_2Cl_2$ mixtures the emission decay became biexponential.[40] Table 1 summarizes steady state luminescence maxima and time resolved luminescence and transient absorbance lifetimes for $CF_3SO_3[pyRe(CO)_3bpy]$ and $\{[(vpy)_2\text{-}vpyRe(CO)_3bpy]\ CF_3SO_3\}_{n\sim200}$ in different experimental conditions.

**Table 1.** Emission maxima and luminescence ($\tau_{em}$) and transient absorption ($\tau_{abs}$) lifetimes for $[pyRe(CO)_3bpy]^+$ and poly-II in different experimental conditions at room temperature. Data taken from ref. 40

| Compound | Solvent | $\lambda_{em}$ / nm | $\tau_{em}$ / ns | $\tau_{abs}$ / ns | $\lambda_{exc}$/nm |
|---|---|---|---|---|---|
| $[pyRe(CO)_3bpy]^+$ | $CH_3CN$ | - | 260 | 282 | 355 |
| | MeOH | - | 218 | 227 | 355[a] |
| | $CH_3CN$ | | - | 225 | 351[b] |
| | $CH_3CN$ | - | 245 | - | 337[c] |
| | DMSO-$CH_3CN$ | 575 | 213 | - | 337 |
| | DMSO-$CH_2Cl_2$ | 569 | 316 | - | 337 |
| | DMSO-water | 574 | 133 | - | 337 |
| poly-II | $CH_3CN$ | - | 226, 53 | 187, <10 | 355 |
| | MeOH | - | 201, 67 | 185 | 355 |
| | $CH_3CN$ | - | - | 184, 35 | 351 |
| | $CH_3CN$ | - | 203 | - | 337 |
| | DMSO-$CH_3CN$ | 577 | 137 | - | 337 |
| | DMSO-$CH_2Cl_2$ | 569 | 143, 31 | - | 337 |
| | DMSO-water | 561 | 440, 83 | - | 337 |

[a]Nd-YAG laser [b]Excimer laser [c]Nitrogen laser

The effect of temperature on luminescence lifetimes also showed a distinctive behavior for $CF_3SO_3[pyRe(CO)_3bpy]$ and poly-II. A monoexponential decay of luminescence in $CH_3CN$ solutions was observed for both $[pyRe(CO)_3bpy]^+$ and poly-II for the entire temperature range (0-65ºC) in study. Moreover, the temperature dependence of emission lifetime is nearly the same for the two compounds.[40] In $CH_3CN$-water (1:4) solutions, however, results were very different for $[pyRe(CO)_3bpy]^+$ and poly-II. The emission decay of $[pyRe(CO)_3bpy]^+$ remains monoexponential between 0ºC and 65ºC, with nearly the same slope, i.e. $\partial\ln(1/\tau)/\partial T$, as in the case of $CH_3CN$ solutions. However, the polymer showed a biexponential behavior at temperatures below 15ºC, with a higher $\partial\ln(1/\tau)/\partial T$ showing a much more marked dependence of $\tau$ on temperatures between 15ºC and 0ºC than between 15ºC and 65ºC.[40]

When poly-II is irradiated with low photonic fluxes, i.e. in steady state or in laser flash irradiations with $n_{hv} \leq 2$ mJ/pulse, only small differences are discerned when the photophysical processes of the MLCT excited state of $-Re(CO)_3bpy^+$ pendants are compared to the photophysical processes of the MLCT excited state in the $CF_3SO_3[pyRe(CO)_3bpy]$ complex. In fact, emission decay lifetimes of both $CF_3SO_3[pyRe(CO)_3bpy]$ and poly-II in $CH_3CN$, calculated from 337 nm flash excitations experiments, are monoexponential and very similar. However, a longer lifetime for the $[pyRe(CO)_3bpy]^+$ ($\tau_{em}$ = 245 ns), compared to poly-II, ($\tau_{em}$ = 203 ns) could be associated to the availability of new deactivation pathways for the MLCT in the polymer due to vibration modes present in the P4VP backbone. This experimental observation and the similarity of $[pyRe(CO)_3bpy]^+$ and the polymer absorption and emission spectra suggest that electronic interactions between Re(I) chromophores in the polymer are negligible in solvents like $CH_3CN$ or DMSO-$CH_3CN$ mixtures. However, this would not be the case for solvents of very low or very high polarity, as in DMSO-$CH_2Cl_2$ and DMSO-water mixtures, respectively. Even though the shape and maxima of emission spectra in DMSO-$CH_2Cl_2$ are nearly the same for $[pyRe(CO)_3bpy]^+$ and the polymer, the polymer experiences a biexponential emission being $\tau_1$ = 143 ns and $\tau_2$ = 31 ns, respectively. Those lifetimes are considerably shorter than that for $[pyRe(CO)_3bpy]^+$, $\tau$ = 316 ns. Moreover, the polymer emission spectrum in DMSO-water is blue-shifted (~ 13 nm) compared to the one of $[pyRe(CO)_3bpy]^+$, and the emission

decay is also biexponential. These photophysical disparities suggest (*vide infra*) that conformational and morphology changes are affecting the photophysical properties of Poly-II, like in the solvent-dependent aggregation observed in a similar polymer, i.e. polystyrene-block-poly(4-vinylpyridine) (PS-b-PVP) functionalized with pendants -Re(CO)$_3$(bpy)$^+$ groups.[35]

Laser flash irradiations with $n_{hv} \geq 12$ mJ/pulse at $\lambda_{ex} = 351$ nm or 355 nm show a very different photophysical behavior for poly-II and CF$_3$SO$_3$[pyRe(CO)$_3$bpy], respectively. $\Phi_{MLCT}$ is nearly three times higher for [pyRe(CO)$_3$bpy]$^+$ than for the polymer.[40] Besides, emission decay for [pyRe(CO)$_3$bpy]$^+$ is monoexponential with a lifetime that is nearly the same as that observed at irradiations with $n_{hv} \leq 2$ mJ/pulse at $\lambda_{ex} = 337$ nm. However, for poly-II, emission decay could only be fitted with two exponentials and the transient generated also experiences a biexponential decay. A fast intrastrand annihilation of MLCT excited states can provide a good explanation for the lower amount of MLCT excited states observed in flash photolysis experiments with the polymer compared to that of the [pyRe(CO)$_3$bpy]$^+$. As in the case of poly-I, this mechanism requires that a large fraction of the photogenerated excited states vanishes within the 20 ns laser pulse. If excited –Re(CO)$_3$bpy$^+$ chromophores are close neighbors and have the correct spatial orientation within the polymer strand, they may undergo a fast annihilation within that period of time. However, using high intensity pulses, a secondary photolysis of the MLCT in the polymer to form intraligand excited states, as discussed above for poly-I, cannot be discarded in this rationalization. Excited chromophores that are disfavored by reason of their position for a fast annihilation or because they do not undergo secondary photolysis will be observed decaying at times longer than 20 ns. The number of these excited chromophores will be higher in flash photolysis experiments with high laser powers (i.e. $\lambda_{ex} = 351$ nm or 355 nm) than in flash photolysis experiments with the low power N$_2$ laser ($\lambda_{ex} = 337$ nm), explaining why 351 nm excitation produces a transient that decays biexponentially and the transient produced after 337 nm excitation decays by first order kinetics. In poly-I, a second order process was observed in addition to the MLCT first order decay (*vide supra*). It should be noted (see Table I) that the longer luminescence lifetime observed after 355 nm or 351 nm excitation is nearly the same as that observed after 337 nm photolysis. The shorter lifetime in 351 nm experiments could be ascribed to the second order processes mentioned before.

## 4. Morphological properties of the polymers

**Poly-II.** The morphologies of poly-**(**II) were studied by transmission electron microscopy (TEM), dynamic light scattering (DLS) and static light scattering (SLS). In TEM studies, the polymer films were obtained by room temperature solvent evaporation of CH$_3$CN solutions of poly-II. When taking photos, the polymer films were not stained with any chemicals, and the contrast of the image in the TEM photos can only originate from the rhenium complexes incorporated to the polymers. The –Re(CO)$_3$bpy$^+$ chromophores in poly-II aggregate and form isolated nanodomains that are dispersed in the polymer matrix film. The dimensions of the nanodomains are between 90 and 430 nm, and they are mainly spherical in shape (Figure 3 a). It should be noted that the dimensions of these nanodomains are considerably larger than the full stretch length of the polymers. As a result, it is likely that the nanodomains contain a considerable number of polymer molecules. Assuming that the mean density of a given nanodomain is the same as that of an isolated poly-II random coil polymer and, neglecting solvation contributions to the hydrodynamic radii, a ratio of around 400 polymer strands constituting a single nanodomain was estimated.[39] When the free pyridines of poly-II are coordinated to CuCl$_2$, the poly-II/CuCl$_2$ polymers aggregate in nanodomains that are distorted from the spherical shape and whose dimensions are smaller than those nanodomains formed by the poly-II (see Figure 3 b). TEM images obtained for poly-II and poly-II/CuCl$_2$ polymers are comparable to the calculated hydrodynamic radii of $156 \pm 6$ nm and $96 \pm 11$ nm from DLS experiments for the aggregates of the poly-II and poly-II/CuCl$_2$ polymers, respectively.[39]
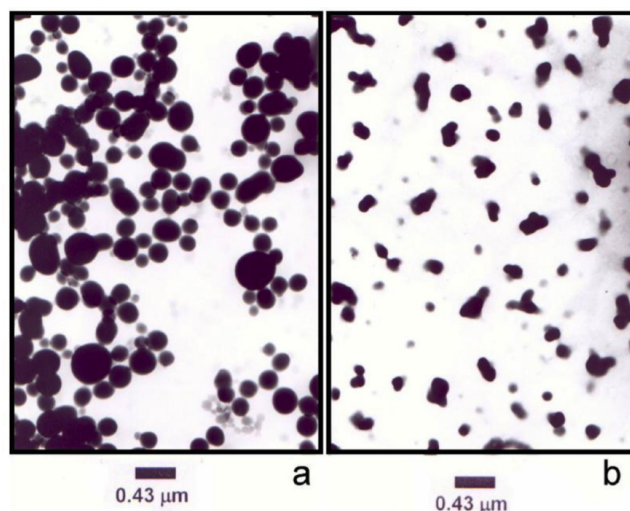
**Figure 3.** Distortion and shrinkage of spherical nanodomains in poly-II polymers after the binding of CuCl$_2$ to the free pyridines of the Re(I) polymer. The Figure shows transmission electron micrographs in solvent cast films of polymers (a) poly-II and (b) poly-II after saturation of the free pyridines with CuCl$_2$. Reprinted with permission from ref. 39. Copyright 2005 American Chemical Society.



**Figure 4.** Transmission electron micrographs in ACN cast films of poly-(III) (top, right and left panels) and poly-(IV) (bottom, right and left panels). Reprinted with permission from ref. 42. Copyright 2006 American Chemical Society.

**Polymers containing mixed pendants.** Poly-III and poly-IV, which contain two different pendants in the strand, i.e., –Re(CO)$_3$(phen)$^+$ and –Re(CO)$_3$(bpy)$^+$, form nanometric aggregates in solution phase. The bimodal relaxation time spectra registered in DLS e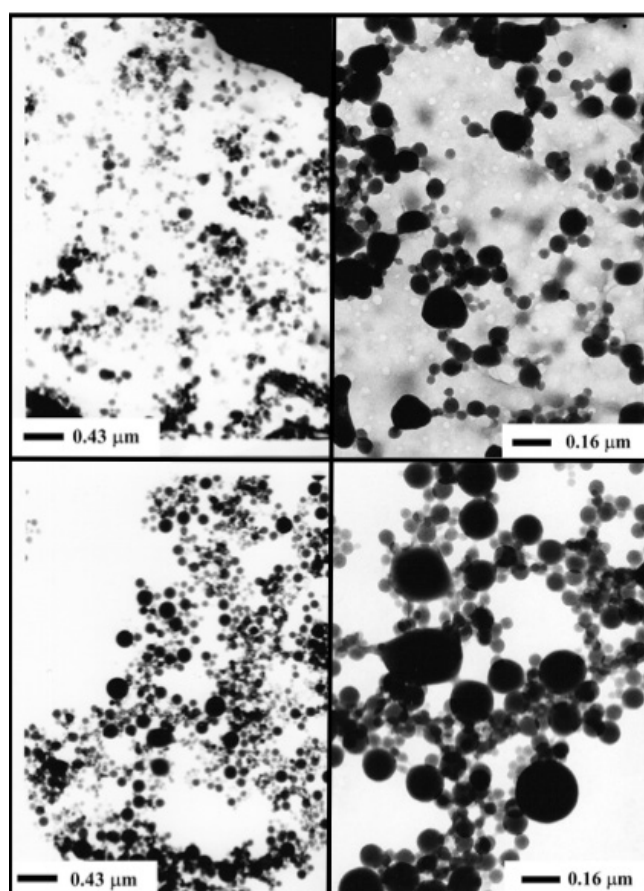xperiments with poly-III and poly-IV reveal the existence of particle sizes between 3 and 14 nm in equilibrium, with bigger particles with radii between 40 and 300 nm. Given the hydrodynamic radius, 221 ± 9 nm for poly-III and 294 ± 5 for poly-IV, the aggregates must be bigger in poly-IV than in poly-III. It appears that the larger the Re(I) load in the polymer, the bigger is the size of the aggregates. TEM images obtained for poly-III and poly-IV also show that the aggregates of poly-IV are larger than those of poly-III. Radii obtained from the DLS experiments are larger than those observed in the TEM micrographs. Similar differences were observed between the DLS hydrodynamic radii and those extracted from the TEM images of poly-II. However, these differences in poly-III and poly-IV are much larger, making the radii determined from TEM images a factor 2 smaller.[41]

**Solvent effects on morphologies: nanoaggregation on polymers poly-V - poly-IX.** The morphologies of poly-V - poly-IX were also studied by TEM.[19] Multiple morphologies of aggregates from these Re(I) polymers were obtained by using different solvents. TEM images of CH$_3$CN and CH$_2$Cl$_2$-cast films of the polymers are shown in Figure 5 and Figure 6, respectively. Polymer morphologies differed when the cast films were obtained either from CH$_3$CN or CH$_2$Cl$_2$ solutions. When the solvent was CH$_3$CN (Figure 6), poly-VI in the solid phase, Re(I) complexes aggregate and form isolated nanodomains that are dispersed in the P4VP backbone. Aggregate dimensions range between 80 and 160 nm, and aggregates are mainly spherical in shape. However, poly-V does not aggregate to form large nanodomains, and only small spherical objects with diameter between 5 and 30 nm are observed. TEM images suggest the formation of aggregates of increasing size when comparing TEM images from poly-VII to poly-IX. The situation is completely different in CH$_2$Cl$_2$. Figure 6 shows TEM images of CH$_2$Cl$_2$-cast films of polymers poly-V - poly-IX. Vesicles were obtained for poly-V, poly-
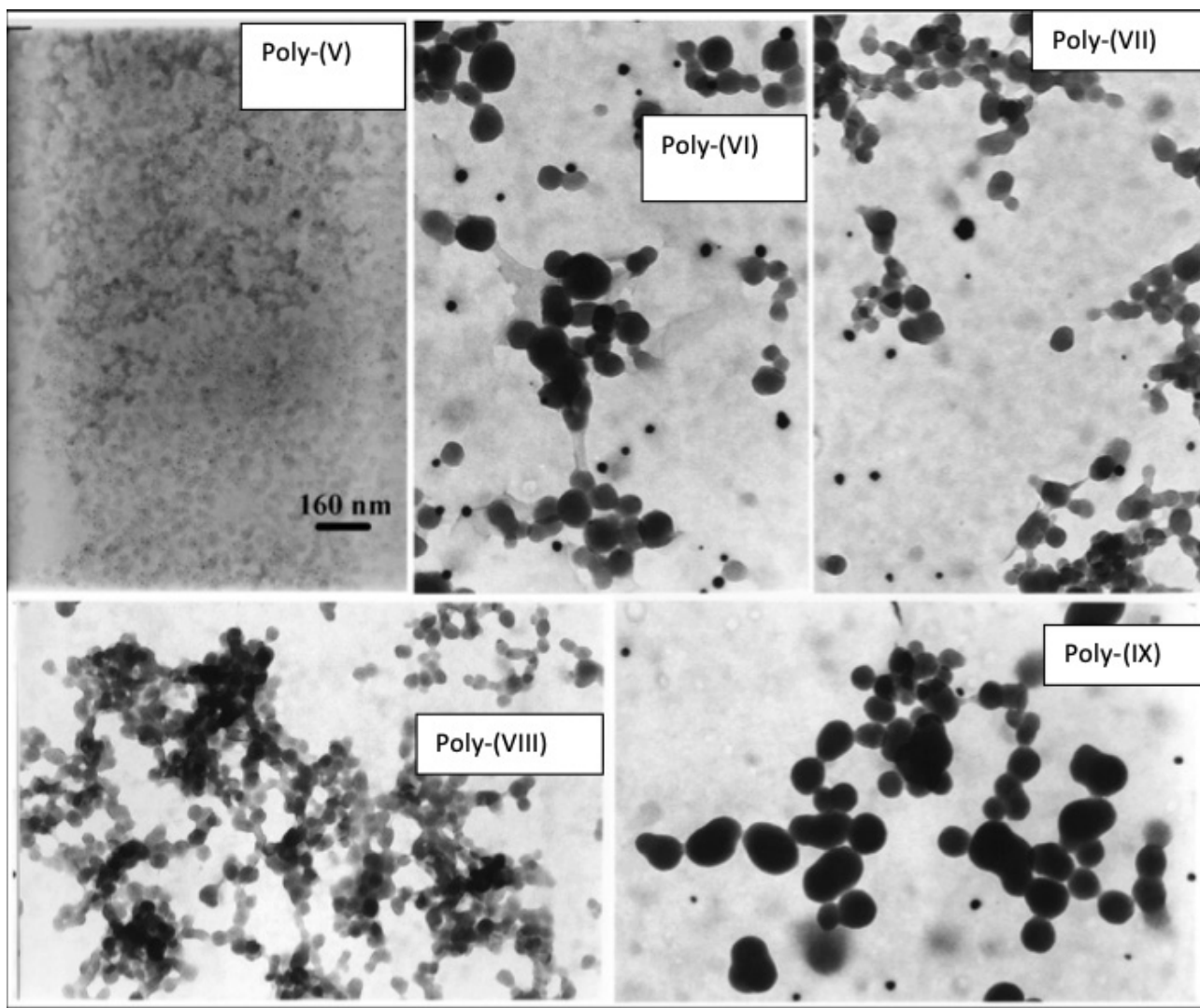


**Figure 5.** Acetonitrile-cast films in polymers poly-(V), poly-(VI), poly-(VII), poly-(VIII) and poly-(IX). The same scale bar applies to all films in the Figure. Reprinted with permission from ref. 19. Copyright 2008 American Chemical Society.

VII, and poly-VIII. The vesicular nature is evidenced by a higher transmission in the center of the aggregates than around their periphery in the TEM pictures. Vescicle sizes are very polydisperse, with outer diameters ranging from 140 nm to large compound vesicles with diameters of up to 1.4 $\mu$m. More interestingly, poly-VI formed branched tubular structures intertwined in a net. The morphologies shown for poly-IX are the intermediate shape of vesicles and tubules. We can rationalize the solvent effect upon aggregation of Re(I) polymers as follows. P4VP is nearly insoluble in $CH_3CN$, but this solvent is a good one for the Re(I) polymers. Then, it is possible that the inner core of the nanodomains present in $CH_3CN$ is formed mainly by the free pyridines of the Re(I) polymers and the outer part is mainly constituted by the solvated Re(I) pendants. The situation is reversed in $CH_2Cl_2$, as this is a good solvent for P4VP. Moreover, poly-(I) and poly-(II) cannot be dissolved in $CH_2Cl_2$, while the solubility of polymers poly-V - poly-IX in this solvent is considerably lower than in $CH_3CN$. In vesicles, however, a pool of $CH_2Cl_2$ molecules may be solvating the uncoordinated pyridines of the polymer in the inner and outer regions of the vesicle, while the Re(I) pendants might be mainly remaining inside the membrane of the vesicle.
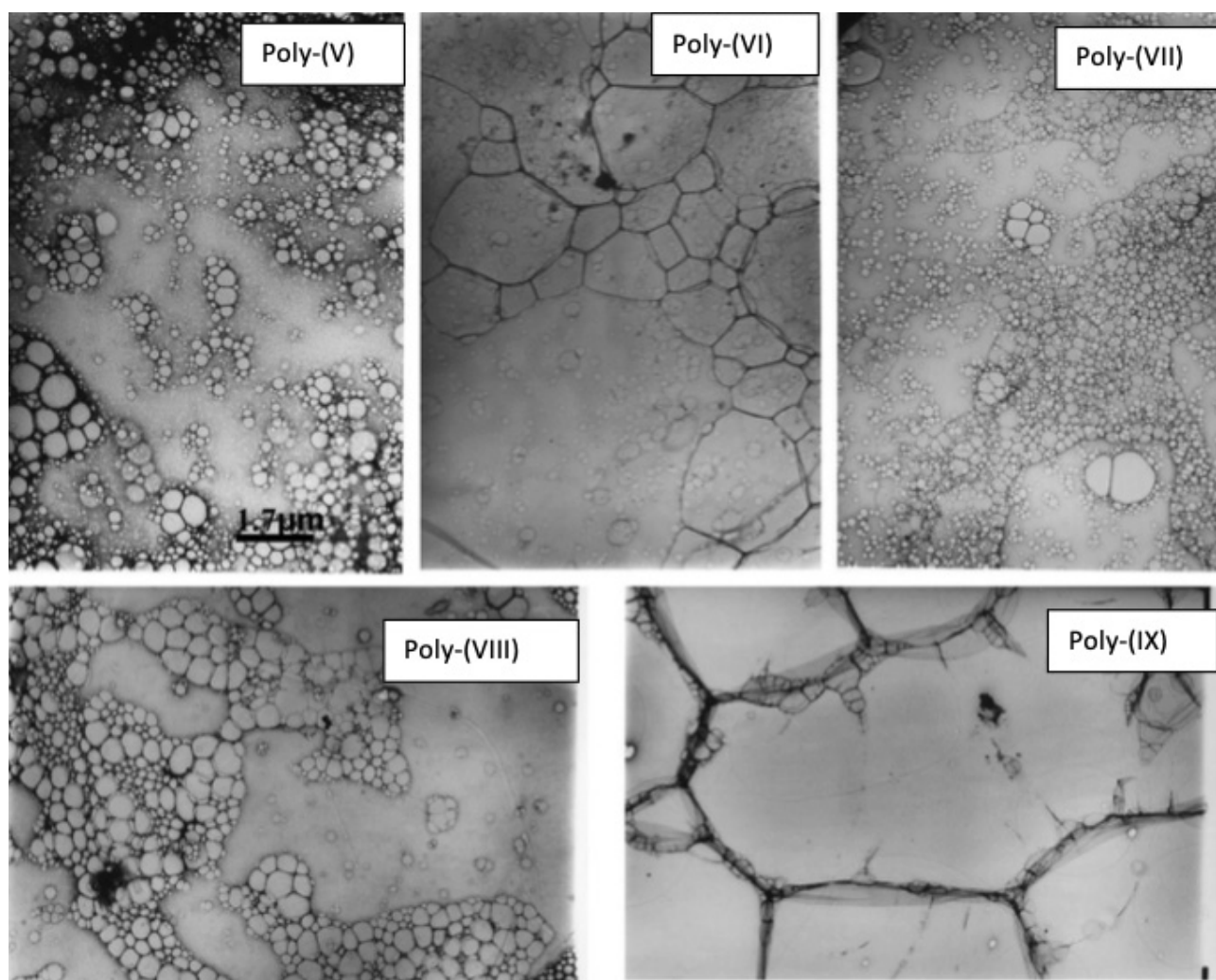


**Figure 6.** Dichloromethane-cast films in poly-(V), poly-(VI), poly-(VII), poly-(VIII) and poly-(IX). The same scale bar applies to all films in the Figure. Reprinted with permission from ref. 19. Copyright 2008 American Chemical Society.

## 5. A correlation between backbone photophysical properties and morphological changes in poly-I

When a deaerated solution of poly-I in $CH_3CN$ is irradiated at $\lambda_{exc}$ = 350 nm, the characteristic luminescence of pendants $-Re(CO)_3phen^+$ chromophores showing a broad unstructured band centered at $\lambda_{max}$ = 550 nm is observed. In this work,[45] a

complementary study to the previous one in the literature,[42] it has been established that the luminescence lifetime of excited $-Re(CO)_3phen^+$ pendant chromophores in poly-I is dependent on the polymer concentration. Luminescence lifetimes were calculated from traces obtained with polymer concentrations corresponding to a total chromophore concentration varying from $[Re] = 2 \times 10^{-5}$M to $4 \times 10^{-4}$M. In the range of $[Re] = 2 \times 10^{-5}$M to $1 \times 10^{-4}$M, a sum of two exponential functions was needed, with lifetimes $\tau_{em,1}$ and $\tau_{em,2}$ to fit the luminescence decay profiles. The dependences of $\tau_{em,1}$ and $\tau_{em,2}$ on the Re chromophore concentration between $2 \times 10^{-5}$M and $4 \times 10^{-4}$M is shown in Figure 7. The shorter lifetime, $\tau_{em,1} = 55 \pm 7$ ns, remains essentially constant between $2 \times 10^{-5}$M and $1 \times 10^{-4}$M, while the longer lifetime, $\tau_{em,2}$, increased monotonically from 240 to 490 ns. When $[Re] > 1 \times 10^{-4}$M, the luminescence decay was fitted without deviation to a single exponential with a lifetime $\tau_{em} = 581 \pm 10$ ns, which is independent of polymer concentration in the concentration range $1 \times 10^{-4}$M $< [Re] < 4 \times 10^{-4}$M.



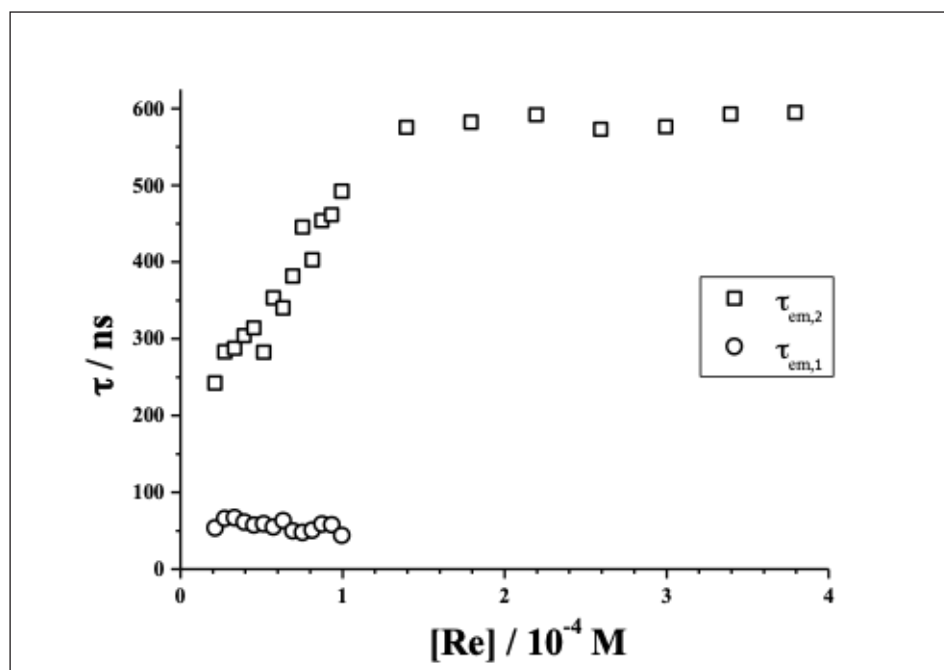**Figure 7.** Dependence of poly-I luminescence lifetimes, $\tau_{em,1}$ and $\tau_{em,2}$, on Re(I) chromophores concentration.

The degree of polymer protonation at different $[HClO_4]/[py]$ ratios was followed by spectrofluorometric techniques. In the steady-state experiments, the total chromophore concentration, $[Re] = 2 \times 10^{-5}$M, was kept constant and the deaerated solutions were irradiated at 350 nm. A large increase in the luminescence of poly-I was observed when Re-free pyridines in poly-I were protonated with $HClO_4$ (Fig. 8), with more than an 8-fold increase in total luminescence. Neither the changes on the band shape nor a band shift accompanied the increase in luminescence quantum yield. The effect of pyridine protonation on poly-I luminescence lifetime was studied at two poly-I concentrations, i.e., $[Re] = 4 \times 10^{-5}$M and $1.6 \times 10^{-4}$M, with $[HClO_4]/[py]$ ratios varying from 0.1 to 1.5. Photophysical observations have shown that these poly-I concentrations are those where the decay of luminescence exhibits biexponential and monoexponential kinetics, respectively. In solutions where $[Re] = 4 \times 10^{-5}$M, luminescence decay kinetics changes from a biexponential regime (when no acid is present) to a mono-exponential law over the whole $[HClO_4]/[py]$ range. A lifetime, $\tau_{em} = 450 \pm 10$ ns, was calculated for the monoexponential decay of the luminescence. When the total concentration of pendants is $1.6 \times 10^{-4}$M, a longer lifetime, $\tau_{em} = 560 \pm 10$ ns, was obtained for luminescence monoexponential decay over the whole range of $[HClO_4]/[py]$ values.
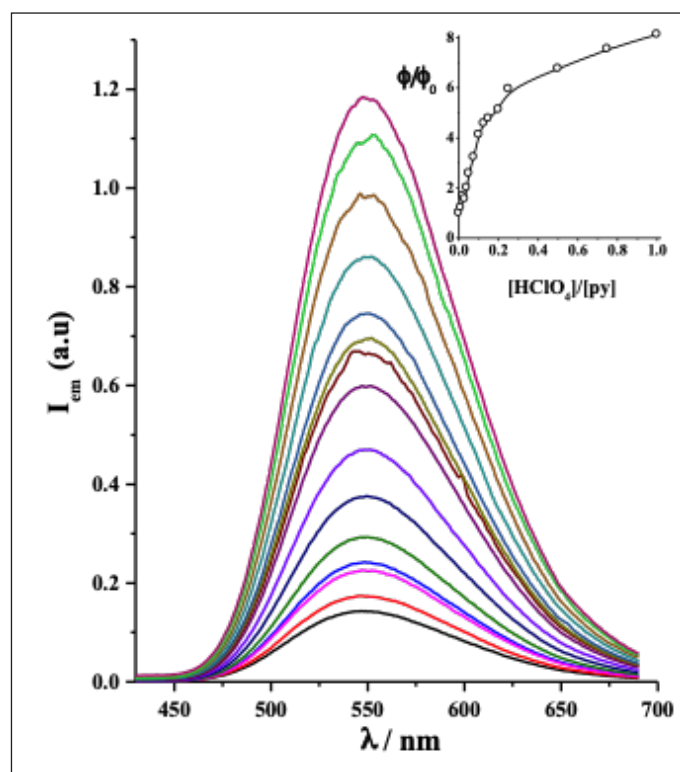
**Figure 8.** Re-P4VP luminescence spectra at different [HClO$_4$]/[py] ratios.
Inset shows the relative increase in luminescence quantum yield as a function of the [HClO$_4$]/[py] ratio. [HClO$_4$]/[py] = 0; 0.01; 0.02; 0.03; 0.04; 0.05; 0.075; 0.10; 0.125; 0.15; 0.20; 0.25; 0.50; 0.75; 1.00.

TEM and AFM studies[45] on poly-I and its protonated form, poly-IH$_n^{n+}$, have shown that (i) the morphology of Re-P4VP polymers is concentration-dependent and (ii) protonation of poly-I polymers alters strongly their morphology. Hereafter, the polymer concentration will be expressed in chromophore units, i.e. [Re]. The morphology of the poly-I at low concentrations ([Re] between 2 x 10$^{-7}$ and 2 x 10$^{-5}$ M, can be described by the coexistence of small objects at polymer scales (diameters below 10 nm) with larger nano aggregates (diameters between 200 and 1000 nm) as well as long fibers at the micrometer scales in a non-homogeneous distribution of aggregate sizes. When polymer concentration is higher ([Re] = 2 x 10$^{-5}$ M), TEM experiments show that poly-I morphology is characterized by nearly spherical nano-domains exhibiting a homogeneous distribution centered at about 25 nm in diameter. After protonation of poly-I, its morphology is strongly affected – at low concentration of the Re(I) polymers, small objects at polymer scales are clearly observed and the fiber-structure is evident; at higher concentration of the Re(I) polymers, polymer morphology shifts after protonation from a homogeneous distribution of spherical nanodomains to a bicontinuous bilayer with attached small objects at polymer scales sizes.[45] Figure 9 shows an example of the morphological changes experienced by poly-I after protonation observed by TEM.

The results have shown that the photophysical and photochemical properties of poly-I and its protonated form are intrinsically associated with medium-imposed polymer morphologies. Those morphological changes have direct impact on the photophysical properties of poly-I polymers and are responsible of (i) the enhancement of luminescence lifetime when increasing polymer concentration and (ii) the nearly 8-fold increase of luminescence quantum yield after protonation of the Re(I) polymer.

The dependence of $\tau_{em,2}$ on polymer concentration, Fig. 7, is another manifestation of the different environments where the luminescent $^3$MLCT excited state is formed. Accordingly, the luminescence decay of poly-I is bi-exponential at [Re] < 1 x 10$^{-4}$M, but it becomes mono-exponential when [Re] > 1 x 10$^{-4}$. Observations made via TEM and AFM show that these environments are the result of a concentration-dependent morphology. Photophysical observations are interpreted, therefore, in terms of medium-destabilized charge-transfer excited states, labeled $^3$MLCT$_{md}$, present in some chromophores within a strand of polymer. $^3$MLCT$_{md}$ excited states may decay to the ground state or they can transfer their excess electronic energy to other chromophores producing medium-stabilized charge-transfer excited states, $^3$MLCT$_{ms}$. The multiple types of aggregates observed with TEM and AFM in poly-I diluted solutions are consistent with the coexistence of $^3$MLCT$_{md}$ and $^3$MLCT$_{ms}$ excited states. By contrast, at higher polymer concentrations, e.g., [Re] = 2 x 10$^{-4}$M, sample inspection using TEM reveals the presence of nearly spherical aggregates with ~25 nm diameters. Therefore,
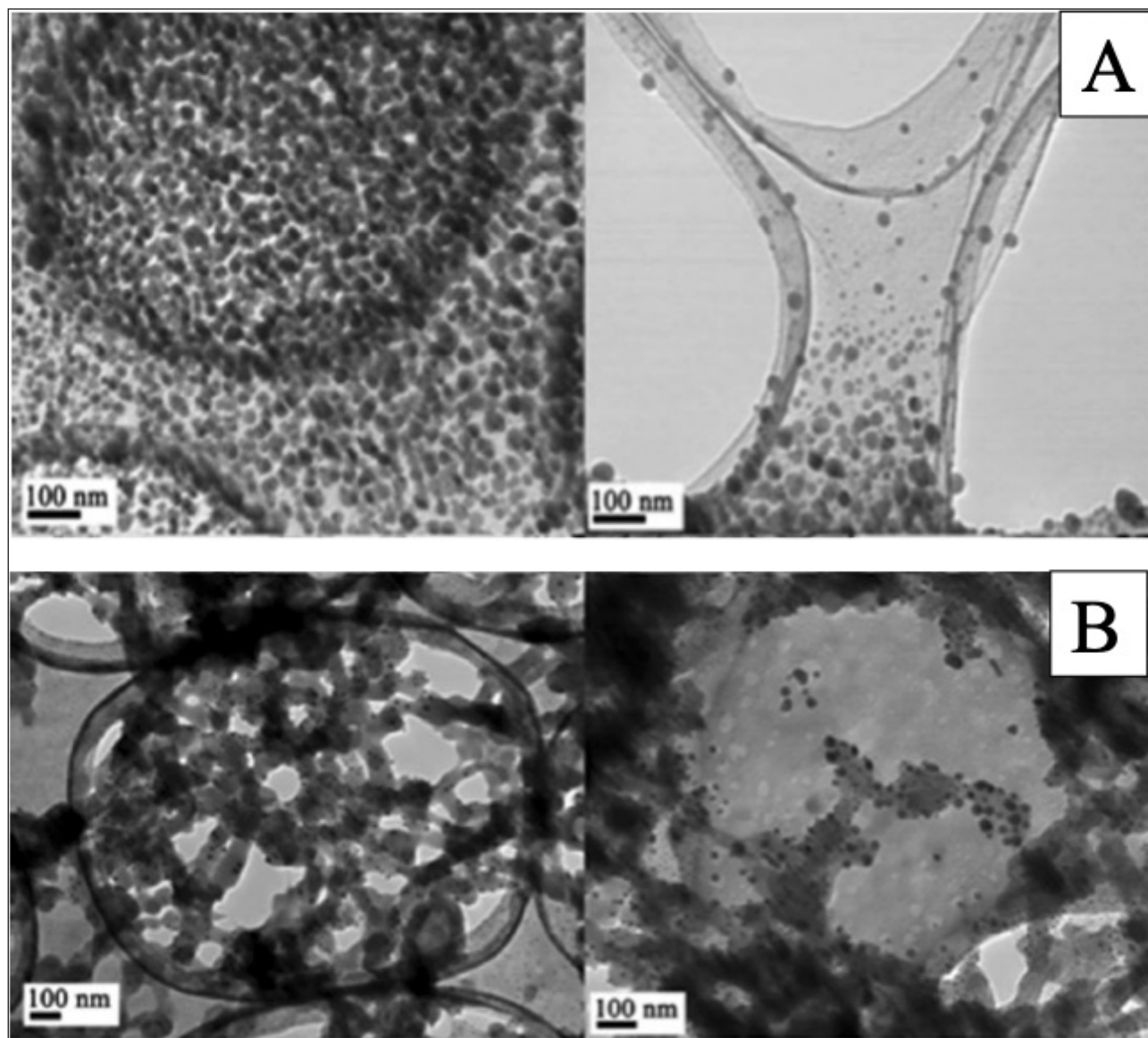
**Figure 9.** (A) TEM images for poly-I. (B) TEM image for poly-IH$_n^{n+}$. Both TEM images were taken from CH$_3$CN cast films of the polymers prepared with [Re] = 2 x 10$^{-4}$. In (B), HClO$_4$ was added to the solution of poly-I with [HClO$_4$]/[py] = 1.5.

some critical mass of polymer between [Re] < 1 x 10$^{-4}$M and [Re] = 2 x 10$^{-4}$M must provide enough material to form the spherical aggregates. Based on the change in the mechanism of the luminescence decay accompanying the formation of spherical aggregates, it can be concluded that the distribution of oligomers when [Re] = 2 x 10$^{-4}$M is more homogeneous than when [Re] = 2 x 10$^{-5}$M. Accordingly, the regime change from a bi-exponential decay to a mono-exponential decay of luminescence is tuned by the concentration-dependent morphology of poly-I. The protonation of the Re(I) polymer induces an 8-fold increase in luminescence quantum yield and a significant increase in $\tau_{em,2}$, from 300 ns to 450 ns for [Re] = 4 x 10$^{-5}$M. Moreover, nearly identical luminescence lifetimes were obtained for the mostly protonated Re(I) polymer and poly-I in the absence of HClO$_4$ acid with solutions having in both cases [Re] = 1.6 x 10$^{-4}$M. These facts suggest that the increase in luminescence quantum yield and lifetime lengthening are the result of morphological changes caused by poly-I protonation in diluted solutions. To some extent, the morphologies of poly-I in concentrated solutions and in diluted acid solutions must be alike or, if they are different, they exert similar perturbations on chromophore photophysics.

**Binding of Cu(II) species and luminescence quenching in poly-II nanoaggregates.** The addition of an acetonitrile solution of CuX$_2$ (X = Cl or CF$_3$SO$_3$) to an acetonitrile solution of the polymer poly-II ([Re] = 8 x10$^{-4}$ M, [py]$_{uncoordinated}$ = 1.5x10$^{-3}$M) produces a rapid coordination of the Cu(II) species to the uncoordinated pyridines poly-II. Binding constant

values of $K_b = 2 \times 10^4$ M$^{-1}$ and $n = 1.8$ and $K_b = 1 \times 10^5$ M$^{-1}$ and $n = 3.0$ were obtained for the binding of CuCl$_2$ or Cu(CF$_3$SO$_3$)$_2$ to the Re(I) polymer, respectively, $n$ being the average size of a binding site.[39] It can be assumed, then, that the complexation of CuCl$_2$ to poly-II proceeds with a lower average coordination number than the complexation of Cu(CF$_3$SO$_3$)$_2$ to the Re(I) polymer, with approximate coordination numbers being 2 and 3, respectively. As noted above (*vide supra*), the binding of Cu(II) to poly-II produces the breakage of the nanoaggregates and yields a wide distribution of particle sizes ranging from a few nanometers at polymer scales to a few hundreds of nanometers covering micelle scales.[39]

The coordination of Cu(II) species to poly-II produces the quenching of the $^3$MLCT excited state by energy transfer processes that are more efficient than those in the quenching of the luminescence of [pyRe(CO)$_3$bpy]$^+$ by Cu(II). Additionally, with poly-II, the kinetics of the quenching by Cu(II) does not follow a Stern-Volmer behavior. Moreover, although in the quenching poly-II luminescence by Cu(CF$_3$SO$_3$)$_2$, the $\Phi_0/\Phi$ ratio shows a sigmoid dependence on Cu(CF$_3$SO$_3$)$_2$ concentration with a limiting value of $\Phi_0/\Phi \sim 6$, the quenching by CuCl$_2$ does not show a plateau on $\Phi_0/\Phi$.[39] Conversely, the reductive redox quenching of the Re(I) polymer's MLCT excited state by TEOA follows a Stern-Volmer kinetics. The striking differences found in the quenching mechanisms with Cu(II) or TEOA are a consequence of the strong chemical interaction (binding) of Cu(II) to the P4VP backbone of the Re(I)-polymer. All quenching processes, either by Cu(II) or TEOA, are more efficient in the polymer than in [pyRe(CO)$_3$bpy]$^+$.[39]

## 6. Resonance energy transfer between –Re(CO)$_3$(tmphen)$^+$ and –Re(CO)$_3$ (NO$_2$-phen)$^+$ pendants in the solution phase photophysics of poly-V, poly-VI, poly-VII, poly-VIII and poly-IX

We have applied ligand substitution reactions of the Re(I) complexes to the derivatization of polymers poly-V, poly-VI, poly-VII, poly-VIII and poly-IX. These polymers consist of a poly-4-vinylpyridine backbone with pendant chromophores –Re(CO)$_3$ (NO$_2$-phen)$^+$ and –Re(CO)$_3$(tmphen)$^+$, with a general formula of $\{[(vpy)_2vpyRe(CO)_3(tmphen)^+]\}_n\{[(vpy)_2vpyRe(CO)_3(NO_2\text{-}phen)^+]\}_m$. The n/m ratio was changed from 9 to 1, maintaining n + m $\sim$ 200. We further studied energy transfer processes between pendant chromophores in these polymers.

**Steady State Photophysics.** Deaerated solutions of polymers poly-V, poly-VI, poly-VII, poly-VIII and poly-IX with total concentration of the Re(I) chromophores equal to or less than $1\times10^{-4}$ M in CH$_3$CN were irradiated at 380 nm to record their emission spectrum. The emission spectrum of poly-V in deoxygenated CH$_3$CN at room temperature exhibited an unstructured band centered at 520 nm. Poly-VI is non-luminescent. Polymers poly-VII, poly-VIII and poly-IX have luminescence spectra, which are the same in shape as that of poly-V. The luminescence quantum yield ($\Phi_{em}$) of poly-V is $\sim 0.03$. Poly-VII has a $\Phi_{em}$ that is nearly $^1/_3$ lower than that of poly-V. $\Phi_{em}$ decreases monotonically from poly-VII to poly-IX. Table 2 summarizes all measured values for $\Phi_{em}$. It shows also the values measured for $\Phi_{em}$ with molar mixtures of polymers poly-V and poly-VI, i.e., to obtain the same $m/(n + m)$ in the mixture as there is in polymers poly-VII, poly-VIII and poly-IX. The values of $\Phi_{em}$ determined for mixtures 90% poly-V + 10% poly-VI, 75% poly-V + 25% poly-VI, and 50% poly-V + 50% poly-VI are noticeably higher than those of poly-VII, poly-VIII and poly-IX, respectively. For instance, while $\Phi_{em}$ for the mixture 50% poly-V + 50% poly-VI is nearly $\frac{1}{2}$ $\Phi_{em}$ for poly-V , $\Phi_{em}$ for polymer poly-IX is nearly 2 orders of magnitude lower than that corresponding to poly-V.[19]

**Table 2.** Photophysical properties of polymers poly-V, poly-VI poly-VII, poly-VIII and poly-IX in acetonitrile at room temperature. Data taken from ref. 19

| | $\phi_D$ [a, b] | $\tau_{fast}$, ns[c] | $\tau_{slow}$, µs[c] | Energy transfer efficiency<br><br>$E_T^j = 1 - \dfrac{\phi_D^j}{\phi_{mb}^j}$ |
|---|---|---|---|---|
| **Polymers** | | | | |
| poly-V | 0.035 | $(7.4 \pm 0.9)\text{x}10^2$ | $3.4 \pm 0.5$ | |
| poly-VI | $< 10^{-4}$ | $0.23 \pm 0.01$[d] | -- | |
| poly-VII | 0.013 | $(1.1 \pm 0.2)\text{x}10^2$ | $1.13 \pm 0.07$ | 0.58 |
| poly-VIII | 0.0038 | $50 \pm 10$ | $0.59 \pm 0.07$ | 0.85 |
| poly-IX | 0.0007 | $< 10$ | $0.047 \pm 0.006$ | 0.94 |
| **Molar blends** | | | | |
| 90% poly-V + 10% poly-VI | 0.031 | | | |
| 75% poly-V + 25% poly-VI | 0.026 | | | |
| 50% poly-V + 50% poly-VI | 0.0125 | | | |

[a] Emission quantum yields of poly-V, poly-VI, poly-VII, poly-VIII and poly-IX. Error ± 10%.

[b] Emission quantum yields, $\phi_D$, measured with molar blends of poly-V and poly-VI in order to obtain the same m/(n+m) in the blend as there is in polymers poly-VII, poly-VIII and poly-IX. Error ± 10%. See text for details.

[c] Obtained from a curve fit analysis with two exponentials from transient absorbance decays in flash photolysis experiments ($\lambda_{ex}$= 351 nm).

[d] Obtained from a transient absorbance monoexponential decay in femtosecond laser photolysis experiments ($\lambda_{ex}$= 387 nm).

**Time-Resolved Absorption Spectroscopy of poly-V, poly-VI, poly-VII, poly-VIII and poly-IX.** Optical excitation of the MLCT absorption bands of the polymers was carried out with a 351 nm excimer laser flash photolysis set-up to record the transient absorption spectra in the 15 ns to microsecond time domain. The transient spectra observed after the 10 ns irradiation of poly-V, poly-VII, poly-VIII and poly-IX solutions in $N_2$-deaerated $CH_3CN$ decayed over a period of several microseconds. A sum of two exponential functions was needed to fit the oscillographic traces with lifetimes $\tau_{fast}$ and $\tau_{slow}$, see Table 2. Transient spectra recorded with either polymer at times immediately after the laser pulse decay, i.e. 20 ns, showed the spectra of the $^3MLCT_{Re\text{-}tmphen}$ excited states decaying by radiative and non-radiative processes.[19] The same spectral features were observed in the generated transients of poly-V, poly-VII, poly-VIII and poly- IX. However, the initial intensity of the spectrum decreases from poly-V, poly-VII, poly-VIII and poly-IX. Since the excited states of poly-VI decayed much faster than the ones of poly-V, poly-VII, poly-VIII or poly- IX, femtosecond techniques were used to record the femtosecond to nanosecond time domain transient absorption spectra of poly-VI. The spectra of the excited states produced ~4 ps after the 387 nm flash irradiation of this polymer consist of three absorption bands, two with maxima at 450 and 600 nm, respectively, and a third one with $\lambda_{max} > 750$ nm.[19] It decays monoexponentially over a period of 1600 picoseconds with a lifetime of 230 ps.[19]

Polymer luminescence decays were also measured in $N_2$-deaerated $CH_3CN$ solutions of poly-V, poly-VII, poly-VIII and poly-IX with $\lambda_{exc}$ = 337 nm. The luminescent profiles of poly-V could be fitted by a single exponential function with a lifetime of $\tau_{em}$ = 5.12 µs. However, the decay of the luminescent profiles for poly-VII, poly-VIII and poly-IX were non-exponential and were fitted following a modification of the Förster treatment, eq. 7:[19]

$$N_t = N_0 \exp\left[-\frac{t}{\tau_D} - a\sqrt{t/\tau_D}\right] \qquad (7)$$

where $N_t$ is the number of molecules that survived excitation at time t, and $\tau_D$ is the excited state lifetime of the donor in the absence of transfer. $a$ is a parameter proportional to the density of acceptor quenching sites which can be calculated according to $a = \frac{4}{3}\pi^{3/2}\rho R_F^3$ where $\rho$ stands for the number of quenching sites per volume and $R_F$ is the Förster critical radius. $N_t$ relates the form of the decay curve to a certain quenching mechanism (in our case Forster's dipole-dipole energy transfer) and two structural quantities, namely quenching site density and critical radius $R_F$. The number of quenching sites within the critical radius is given by $N = \frac{a}{\sqrt{\pi}}$.

Poly-VII, poly-VIII and poly-IX luminescence decay profiles were fitted using Equation 7 with the values of $a = 1.90$, 4.6 and 19.3, respectively, and $\tau_D = 5.12$ µs.[19] Values of $N \approx 1.1$; 2.6 and 11 can be calculated for poly-VII, poly-VIII and poly-IX using the vales of $a = 1.90$, 4.6 and 19.3, respectively. A calculation of $R_F$ for the present system gives a value of 10.7 Å.[19] Using this value of $R_F$ and the values of $a$ obtained above from the luminescence decay fitting, values of $\rho = 2.1 \times 10^{-4}$, $5.05 \times 10^{-4}$ and $2.1 \times 10^{-3}$ $N_{acceptors}/Å^3$ can be calculated for polymers poly-VII, poly-VIII and poly-IX, respectively. These numbers compared well with the number of quenching neighbors estimated roughly from a molecular modeling of the polymers.[19]

From the comparison of $\Phi_{em}$ values for polymers poly-VII, poly-VIII and poly-IX with the corresponding $\Phi_{em}$ of the molar blends 90% poly-V + 10% poly-VI, 75% poly-V + 25% poly-VI, and 50% poly-V + 50% poly-VI, it can be inferred that the substitution of pendants $Re(CO)_3(tmphen)^+$ by pendants $Re(CO)_3(NO_2\text{-phen})^+$ in the P4VP backbone produces a decrease in $\Phi_{em}$ that is in proportion to the number of $Re(CO)_3(NO_2\text{-phen})^+$ pendants relative to that of $Re(CO)_3(tmphen)^+$ pendants due to an energy transfer process that involves the excited states $MLCT_{Re \to tmphen}$ and $MLCT_{Re \to NO2\text{-phen}}$.

$\Phi_{em}$ of the molar blends 90% poly-V + 10% poly-VI, 75% poly-V + 25% poly-VI, and 50% poly-V + 50% poly-VI can be compared to the $\Phi_{em}$ values that would have been expected for polymers poly-VII, poly-VIII and poly-IX if no energy transfer between $-[Re(CO)_3(tmphen)^+]^*$ and $-Re(CO)_3(NO_2\text{-phen})^+$ pendants had occurred, eqs. 10-11:

$$\Phi_D = \left(\frac{A}{A_T}\right)\Phi_D{}^0 \qquad\qquad (10)$$

$$\frac{A}{A_T} = \frac{n\varepsilon_{\lambda,n}}{n\varepsilon_{\lambda,n} + m\varepsilon_{\lambda,m}} \qquad\qquad (11)$$

Where $A$ is the absorbance of donor $-Re(CO)_3(tmphen)^+$ at wavelength $\lambda$, $A_T$ is the total absorbance of the solution, and $\varepsilon_{\lambda,n}$ and $\varepsilon_{\lambda,n}$ are the molar extinction coefficients of donor $-Re(CO)_3(tmphen)^+$ and acceptor $-Re(CO)_3(NO_2\text{-phen})^+$ at wavelength $\lambda$, respectively, and $\Phi_D{}^0$ is the emission quantum yield of the donor, i.e. 0.0347 for poly-V. Given the values of $5.5 \times 10^5$ and $7.8 \times 10^5$ $M^{-1}cm^{-1}$ for the extinction coefficients of poly-V and poly-VI at 380 nm, $\Phi_D$ values of 0.0298, 0.0236 and 0.0142 can be calculated for poly-VII, poly-VIII and poly-IX, respectively. Those $\Phi_D$ values are similar to the experimental values measured for the molar blends 90% poly-V + 10% poly-VI, 75% poly-V + 25% poly-VI, and 50% poly-V + 50% poly-VI, which are 0.031, 0.026 and 0.0125, respectively (see Table 2). Therefore, it can be concluded that there is no bimolecular (i.e. intermolecular) quenching between excited $-Re(CO)_3(tmphen)^+$ chromophores in polymers poly-V and acceptors $-Re(CO)_3(NO_2\text{-phen})^+$ in polymers poly-VI in the blends.

Regarding the energy transfer process that quenches progressively the emission of the excited $-Re(CO)_3(tmphen)^+$ (donor D) pendants with the increasing number of $-Re(CO)_3(NO_2\text{-phen})^+$ (acceptor A) pendants in polymers poly-VII, poly-VIII and poly-IX, the crucial point is that, when passing from polymer poly-VII to poly-VIII and then to poly-IX, the probability of a donor D to be in the vicinity of an acceptor A increases.

Energy transfer efficiency between D and A in polymers poly-VII, poly-VIII and poly-IX can be calculated according to:

$$E_T^j = 1 - \frac{\Phi_D^j}{\Phi_{mb}^j} \qquad\qquad (12)$$

where $E_T^j$ represents energy transfer efficiency in polymer $j$ [$j$ = poly-VII, poly-VIII and poly-IX], $\Phi_D^j$ represents emission quantum yields for polymers poly-VII, poly-VIII and poly-IX, and $\Phi_{mb}^j$ are the emission quantum yields of the molar blends 90% poly-V + 10% poly-VI, 75% poly-V + 25% poly-VI, and 50% poly-V + 50% poly-VI, respectively. The experimental $E_T^j$ values for polymers poly-VII, poly-VIII and poly-IX are 0.58, 0.85 and 0.94 respectively (Table 2).

Taking the $E_T^j$ calculated above for polymers poly-VII, poly-VIII and poly-IX, mean values for the energy transfer rate constant between $\text{MLCT}_{\text{Re} \to \text{tmphen}}$ and $\text{MLCT}_{\text{Re} \to \text{NO2-phen}}$ can be calculated in these polymers with the aid of Equation 13:
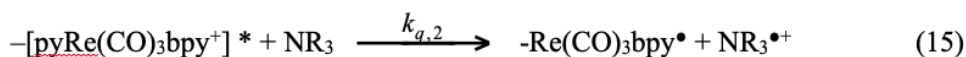
$$\overline{k_{ET}} = \frac{1}{\tau_D}\left( \frac{E_T^j}{1 - E_T^j} \right) \qquad\qquad (13)$$

The values of $\overline{k_{ET}}$ obtained for polymers poly-VII, poly-VIII and poly-IX are $2.7 \times 10^5$, $1.1 \times 10^6$ and $3.1 \times 10^6$ s$^{-1}$, respectively. It should be noted that those $\overline{k_{ET}}$ values are only average contributions in the polymers.[19]

## 7. MLCT luminescence quenching by amines: aggregation decreases the reorganization energy favoring the observation of the Marcus inverted effect

Understanding the factors that determine electron-transfer (*ET*) rates is of considerable importance, due to *ET* ubiquity and the essential roles it plays in many physical, chemical and biological processes. Different factors govern the kinetics of *ET* reactions, such as solvent environment, free energy of reaction ($\Delta G$) and electronic coupling. *ET* rates should follow a parabolic dependence on $\Delta G$ according to the remarkable prediction of Marcus theory. In the classical limit, the theory predicts a bell-shaped Gibbs energy-rate relationship for reactions in condensed media: rate constants are expected to be small for weakly exothermic reactions, increase to a maximum for moderately exothermic reactions (the *normal region*), and decrease for highly exothermic electron transfer reactions in the so-called *inverted region*. Due to the lack of the experimental evidence, a lot of controversy was generated by the theoretical prediction of this *inverted region*. In fact, the confirmation of the *inverted effect* took a lapse of about 25 years after its postulation. After that, the *inverted region* has been observed experimentally in many electron transfer systems.[37] Experimental evidence for the Marcus *inverted region* in the bimolecular *ET* reactions is, however, very rare.[49] In most bimolecular *ET* reactions, mainly due to the influence of the diffusional rate of the reactants on the effective reaction rates, the variation in the *ET* rates with the $\Delta G$ of the reactions follows the Rehm-Weller type of behavior.[50] There are two main obstructions to observing the Marcus inverted region in bimolecular ET reactions, namely, (i) diffusion of the reactants and (ii) lack of availability of suitable donor–acceptor series to achieve very high reaction exothermicities. The first shortcoming may be reduced if *ET* is carried out in systems where reactants are confined into micelles and/or nano aggregates where their movements may be highly restricted. We decided to test the ability of our polymers in their aggregates to overcome the first drawback. Thus, we decided to compare $^3$MLCT luminescence quenching of $-\text{Re(CO)}_3\text{bpy}^+$ chromophores by amines in poly-II with the $^3$MLCT luminescence quenching of $[\text{pyRe(CO)}_3\text{bpy}]^+$ chromophores by the same amines, in order to see if the formation of nano aggregates in poly-II (*vide supra*) could have any effect on quenching kinetics behavior.

**Forward electron transfer.** The reductive quenching of the $^3$MLCT excited state of $[\text{pyRe(CO)}_3\text{bpy}]\text{CF}_3\text{SO}_3$ and poly-II by amines produces the oxidized form of the amine and the reduced radical of the rhenium complex; eqs. 14,15

$$[\text{pyRe(CO)}_3\text{bpy}^+]^* + \text{NR}_3 \xrightarrow{k_{q,1}} \text{pyRe(CO)}_3\text{bpy}^\bullet + \text{NR}_3^{\bullet+} \qquad (14)$$

$$-[\text{pyRe(CO)}_3\text{bpy}^+]^* + \text{NR}_3 \xrightarrow{k_{q,2}} -\text{Re(CO)}_3\text{bpy}^\bullet + \text{NR}_3^{\bullet+} \qquad (15)$$

where $[\text{pyRe(CO)}_3\text{bpy}^+]^*$ and $-[\text{Re(CO)}_3\text{bpy}^+]^*$ denote the MLCT excited states in $\text{pyRe(CO)}_3\text{bpy}^+$ and in a pendant $-\text{Re(CO)}_3\text{bpy}^+$ chromophore of poly-II, and $k_{q,1}$ and $k_{q,2}$ denote the bimolecular rate constants for $\text{pyRe(CO)}_3\text{bpy}^+$ and poly-II, respectively.

The results of the quenching experiments are shown in Table 3. The data were plotted according to the Stern-Volmer equation; eq. 16

$$\frac{\tau_0}{\tau} = 1 + k_q\tau_0\left[\text{NR}_3\right] \qquad\qquad (16)$$

where $\tau_0$ is the excited state lifetime in the absence of quencher and $\tau$ is the luminescence lifetime in the presence

of quencher. The plots were linear over the range of quencher concentrations used and the intercepts were unity as expected.[37] $k_q$ values, collected in Table 3, were determined from the slopes of the lines using $\tau_0$ = 245 and 203 ns for $[pyRe(CO)_3bpy]CF_3SO_3$ and poly-II, respectively.[37]

**Table 3.** Quenching rate constants ($k_q \pm$ 2 SE) of MLCT excited states of poly-II and $pyRe(CO)_3(bpy)^+$ in acetonitrile by aliphatic and aromatic amines. Data taken from ref. 37

| | | | Poly-II | $pyRe(CO)_3(bpy)^+$ |
|---|---|---|---|---|
| Quencher | $E_{1/2}$, V(vs. SCE) | $\Delta G/eV$ | $k_q/M^{-1}s^{-1}$ | $k_q/M^{-1}s^{-1}$ |
| N,N,N',N'-tetramethyl 1,4-phenylenediamine | 0.12 | -1.16 | $(4.8\pm0.8) \times 10^9$ | $(2.0\pm0.2) \times 10^{10}$ |
| 1,4-phenylenediamine | 0.26 | -1.02 | $(1.1\pm0.6) \times 10^{10}$ | $(1.3\pm0.1) \times 10^{10}$ |
| 1,2-phenylenediamine | 0.40 | -0.88 | $(1.5\pm0.1) \times 10^{10}$ | $(1.30\pm0.04) \times 10^{10}$ |
| DABCO | 0.56 | -0.72 | $(7.8\pm0.8) \times 10^9$ | $(1.02\pm0.02) \times 10^{10}$ |
| N,N,N',N'-tetramethylethylenediamine | 0.87 | -0.41 | $(2.1\pm0.6) \times 10^9$ | $(1.0\pm0.2) \times 10^9$ |
| N,N di-isopropyl-ethylamine | 0.89 | -0.39 | $(6\pm1) \times 10^9$ | $(5\pm1) \times 10^9$ |
| Aniline | 0.93 | -0.35 | $(6.7\pm0.4) \times 10^9$ | $(5.5\pm0.4) \times 10^9$ |
| Triethylamine | 0.99 | -0.29 | $(2.1\pm0.2) \times 10^9$ | $(1.00\pm0.06) \times 10^9$ |
| N,N,N',N'-tetramethyl-diaminomethane | 1.06 | -0.22 | $(5\pm1) \times 10^8$ | $(2.45\pm0.06) \times 10^8$ |
| Diethylamine | 1.14 | -0.14 | $(1.3\pm0.2) \times 10^8$ | $(1.4\pm0.2) \times 10^8$ |
| Di-isopropylamine | 1.31 | 0.03 | $(1.1\pm0.2) \times 10^8$ | $(2.6\pm0.2) \times 10^7$ |
| Dibencylamine | 1.36 | 0.08 | $(8\pm1) \times 10^6$ | $(8\pm1) \times 10^6$ |
| n-butylamine | 1.39 | 0.11 | $(1.3\pm0.1) \times 10^7$ | $(6\pm1) \times 10^6$ |

**Electron transfer mechanism.** The following kinetic scheme may be considered for the forward electron transfer reaction:[37]

$$(A^+)^* + D \xrightarrow[k_{-d}]{k_d} [(A^+)^*, D] \xrightarrow[k_{-e}]{k_e} [(A^\bullet), D^{\bullet+}] \xrightarrow{k_p} A^\bullet + D^{\bullet+} \qquad (17)$$
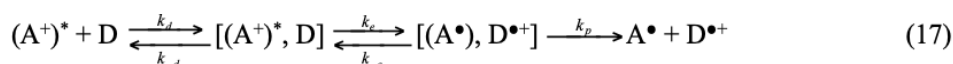
where $k_d$ is the diffusion rate constant, $k_{-d}$ is the dissociation rate constant, $k_e$ and $k_{-e}$ are the forward and backward electron transfer rate constants, and $k_p$ is the rate constant for pair separation. $(A^+)^*$ that represents the acceptor (i.e. $pyRe(CO)_3(bpy)^+$ and/or pendants $-Re^I(CO)_3(bpy)^+$ in poly-II) in its MLCT excited state and D the amine donor.

Under the assumption that $k_p$ is much larger than $k_{-e}$, which is supported by the observation of the $-Re^I(CO)_3(bpy)^\cdot$ radical species by flash photolysis experiments,[37] the overall rate constant may be approximately written as:

$$k_q = \frac{k_d}{1 + \dfrac{k_{-d}}{\kappa\nu_N}\exp\left(\dfrac{\Delta G^*}{RT}\right)} \qquad (18)$$

where $\kappa$ is the transmission coefficient of electron transfer, which is 1 in the classical limit, and $\nu_N$ is the frequency factor, which varies from the order of $10^{12}$ to $10^{14}$ s$^{-1}$ and can be approximated to be of the order of $10^{13}$ s$^{-1}$. $\Delta G^*$ is the activation free energy for the electron-transfer step.

Several relationships between $\Delta G^*$ and $\Delta G$ have been proposed. In the classical parabolic Marcus equation, $\Delta G^*$ becomes (eq. 19):

$$\Delta G^* = \frac{(\lambda + \Delta G)^2}{4\lambda} \qquad (19)$$

where $\lambda/4$ is the activation free energy when $\Delta G = 0$ (intrinsic barrier). Here $\lambda$, the total reorganization energy, is considered to be the sum of the inner-sphere ($\lambda_{in}$) and solvent ($\lambda_{out}$) contributions:

$$\lambda = \lambda_{in} + \lambda_{out} \tag{20}$$

The solvent reorganization energy may be estimated by:

$$\lambda_{out} = e^2 \left( \frac{1}{2r_D} + \frac{1}{2r_A} - \frac{1}{r_{DA}} \right) \left( \frac{1}{n^2} - \frac{1}{\varepsilon} \right) \tag{21}$$

where $r_D$ and $r_A$ are the radii of the donor and acceptor, $r_{DA}$ is the distance between donor and acceptor in the encounter complex, $n$ is the refractive index of the solvent, and $\varepsilon$ is the solvent dielectric constant. Using a mean value of $r_D$ for all amines and a value of $r_A = 8$Å for pyRe(CO)$_3$(bpy)$^+$ from interatomic distances obtained from similar related Re(I) compounds, a value of 0.7 eV may be estimated for $\lambda_{out}$.[37]

The diffusion rate constant ($k_d$), calculated according to Smoluchowski for non-charged molecules, has a value of 2.0 $\times 10^{10}$ M$^{-1}$s$^{-1}$ in acetonitrile.[37] Following the Fuoss and Eigen equation, $K_d$, i.e., the equilibrium constant of the encounter complex ($K_d = k_d/k_{-d}$), may be estimated as 5.4 M$^{-1}$ and hence $k_{-d} = 3.7 \times 10^9$s$^{-1}$.

However, in order to fit the experimental results for bimolecular charge separation reactions where the inverted effect predicted by the parabolic Marcus expression is not observed and asymptotic behavior is obtained for $k_q$ at higher exoergonic reactions, an expression of $\Delta G^*$ that tends asymptotically toward zero for highly negative values of $\Delta G$ is necessary. The Rehm-Weller relationship, eq. 22, meets this requirement.

$$\Delta G^* = \frac{\Delta G}{2} + \left[ \left( \frac{\Delta G}{2} \right)^2 + \left( \frac{\lambda}{4} \right)^2 \right]^{1/2} \tag{22}$$

**Relationship between rate constants and $\Delta G$.** The experimental values of $k_{q,1}$ and $k_{q,2}$ are plotted against $\Delta G$ in Figure 10. The rate constant for luminescence quenching of pyRe(CO)$_3$(bpy)$^+$, $k_{q,1}$, increases as the driving force becomes less positive, i.e. -0.6 eV $< \Delta G <$ 0.2 eV. Eventually, it reaches the diffusional value, $k_d$, when -1.2 eV $< \Delta G <$ -0.7, and for more negative values of $\Delta G$, an asymptotic plateau is obtained. Luminescence quenching of poly-II shows a similar behavior: $k_{q,2}$ increases as $\Delta G$ varies between 0.2 and -0.7 eV and it reaches the diffusional value at $\Delta G \sim$ -0.9 eV. However, at more negative values, it shows "vestiges" of inverted region behavior. At $\Delta G =$ -1.15 eV, $k_{q,2}$ is 4.8 x10$^9$ M$^{-1}$s$^{-1}$, i.e. slightly lower than $k_d$. This is a situation that is often encountered in studies of bimolecular electron transfer reactions at high exoergonic reactions. A comparison of the values of $k_{q,1}$ and $k_{q,2}$ shown in Table 3 indicates that, in general, $k_{q,2}$ is slightly higher than $k_{q,1}$ for values of -0.6 eV $< \Delta G <$ 0.2 eV. For $\Delta G <$ -0.7 eV, this situation is reversed and $k_{q,1}$ becomes higher than $k_{q,2}$. In fitting experimental $k_q$ values with either Marcus and/or Rehm-Weller model for $\Delta G^*$, it was observed that $k_{q,1}$ values were better fitted by the Rehm-Weller model (Figure 10d), while $k_{q,2}$ values were better represented by the Marcus model (Figure 10a) for $\Delta G^*$, as it is suggested by the correlation coefficients shown in Table 4 and Figure 10. Figures 10a, b, c and d show the best fitting of experimental data points to the Marcus and Rehm-Weller expression of $\Delta G$ using eqs. 18, 19 and eqs. 18, 22, respectively. The best fit was obtained using a $k_d = 2 \times 10^{10}$ M$^{-1}$s$^{-1}$ and the values of $\kappa$ and $\lambda$ collected in Table 4.

**Table 4.** Transmission electron coefficients ($\kappa$) and total reorganization energy ($\lambda$) for MLCT luminescence quenching of pyRe(CO)$_3$(bpy)$^+$ and poly-II by amines. R stands for the correlation coefficient for each fit of the experimental values of k$_q$ for pyRe(CO)$_3$(bpy)$^+$/ poly-II with Marcus and/or Rehm-Weller models of $\Delta$G*. Data taken from ref. 37

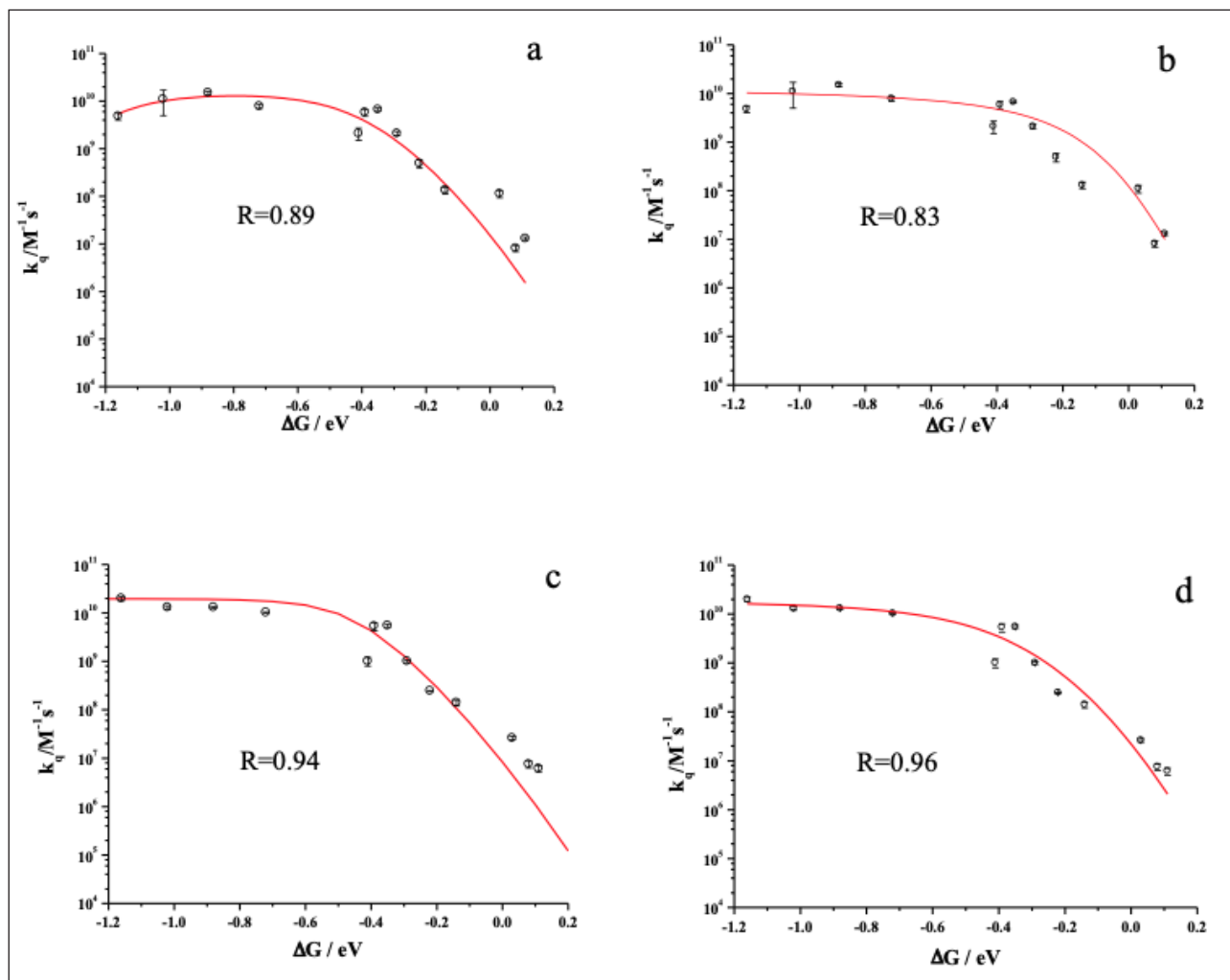| System | Model for $\Delta G^*$ | $\kappa$ | $\lambda$/eV | R |
|---|---|---|---|---|
| pyRe(CO)$_3$(bpy)$^+$ | Marcus | $(2 \pm 1)$ x $10^{-2}$ | $1.2 \pm 0.1$ | 0.94 |
| | Rehm-Weller | $(2 \pm 1)$ x $10^{-2}$ | $1.1 \pm 0.2$ | 0.96 |
| Poly-II | Marcus | $(7 \pm 1)$ x $10^{-4}$ | $0.80 \pm 0.03$ | 0.89 |
| | Rehm-Weller | $(9 \pm 5)$ x $10^{-4}$ | $0.6 \pm 0.2$ | 0.83 |

**Figure 10.** Quenching rate constant dependence on $\Delta G$ for MLCT luminescence quenching by amines. Figures 10 (a, b) show $k_{q,2}$ vs. $\Delta G$ for poly-II. The solid line in Fig. 10a shows the best fitting of experimental data points to the Marcus expression of $\Delta G$, while the solid line in Fig. 10b shows the best fitting of experimental data points to the Rehm-Weller expression of $\Delta G$. Figures 10 (c, d) show $k_{q,1}$ vs. $\Delta G$ for $pyRe(CO)_3(bpy)^+$. The solid line in Fig. 10c shows the best fitting of experimental data points to the Marcus expression of $\Delta G$, while the solid line in Fig. 10d shows the best fitting of experimental data points to the Rehm-Weller expression of $\Delta G$. The values of $\kappa$ and $\lambda$ obtained by the curve fit analysis of Figs. 10 a, b, c and d are collected in Table 5. R stands for the regression coefficient.

Even though the Marcus model for poly-II seems to better describe the $k_q$ relationship with $\Delta G$ and the Rehm-Weller model seems to be better for $pyRe(CO)_3(bpy)^+$, there are two features in which both models are coincident: (i) total reorganization energy ($\lambda$) is higher by about 0.3-0.5 eV for $pyRe(CO)_3(bpy)^+$ than for poly-II; (ii) the quenching reaction of MLCT by amines is a non-adiabatic reaction ($\kappa \sim 1 \times 10^{-3}$-$1 \times 10^{-2}$). It is important to recall, at this point, that TEM and DLS studies on poly-II demonstrated that $Re^I$ polymer molecules aggregate to form spherical nanoaggregates of radius $R \sim 156$ nm (*vide supra*). The fact that the motion of solvent molecules is retarded by several orders of magnitude in restricted media such as micelles or aggregates, compared to that in homogeneous solvents, is a well-known fact. Thus, solvent reorganization may not be contributing entirely within the time scale of the electron transfer reaction between poly-II MLCT and amines. Higher values of $\lambda$ are thus expected for $pyRe(CO)_3(bpy)^+$ than for poly-II, see Table 4. For $\Delta G < \lambda$, the limiting value of $\Delta G^*$ from Equation 19 tends to $\Delta G^* \sim \frac{1}{2}(\Delta G) + \frac{1}{4}(\lambda)$. Since $\lambda$ is higher for $pyRe(CO)_3(bpy)^+$ than for poly-II, then $k_{q,2} \geq k_{q,1}$. However, vibrational modes of uncomplexed pyridines in the polymer backbone may be contributing to a decrease of $\lambda_{in}$, explaining the fact that $k_{q,2} \geq k_{q,1}$ for most of the amines studied. Nonetheless, since the amine might have a certain tendency to be close to the polymer by hydrogen bonding interactions with the free pyridine groups, the amine molecules diffusion to form the encounter complex with the $-Re(CO)_3(bpy)^+$ chromophore may be favored, compared to $pyRe(CO)_3(bpy)^+$, explaining a higher value of $k_q$ in poly-II than in $pyRe(CO)_3(bpy)^+$. There might be a simultaneous contribution of these three effects for $k_{q,2} \geq k_{q,1}$ in the normal region. In the inverted region ($-\Delta G > \lambda$) for higher exothermic quenching reactions, the absence of a solvent reorganization in the quenching of poly-II MLCT luminescence by amines may explain a slight tendency of $k_{q,2}$ to decrease while $k_{q,1} \sim k_d$.

## Conclusions

Polymers derived from P4VP with attached $-Re(CO)_3(N^N)^+$ pendants show remarkable differences in their photophysical and photochemical properties when compared to the single $LRe(CO)_3(N^N)$ molecules, mainly due to two distinctive properties: (i) the proximity of metallic centers in the polymers, which allows the observation of annihilation processes of the excited states that are not observed in diluted solutions of the single $fac$-$LRe(CO)_3(N^N)$ molecules, and (ii) the solvent/temperature dependent aggregation of polymer strands that impose different morphologies, which ultimate deeply affect the photophysical properties of the attached $-Re(CO)_3(N^N)^+$ pendants. In addition, and connected to (ii), a retardation of the molecular motion due to the restricted media might favor the observation of the Marcus *inverted effect* in bimolecular reactions due to the fact that low values of the solvent reorganization energies may be achieved within aggregates.

## Acknowledgements

## References

[1] Vlček, A.: Ultrafast Excited-State Processes in Re(I) Carbonyl-Diimine Complexes: From Excitation to Photochemistry. In *Photophysics of Organometallics*; Lees, A. J., Ed.; Topics in Organometallic Chemistry; Springer Berlin / Heidelberg, 2010; Vol. 29; pp 73-114.

[2] Fox, M. A.; Chanon, M. *Photoinduced Electron Transfer; Elsevier, Amsterdam, 1988.*

[3] Balzani, V.; Bolletta, F.; Gandolfi, M.; Maestri, M.: Bimolecular electron transfer reactions of the excited states of transition metal complexes. In *Organic Chemistry and Theory*; Topics in Current Chemistry; Springer Berlin / Heidelberg, 1978; Vol. 75; pp 1-64.

[4] Grätzel, M. *Energy Resources Through Photochemistry and Catalysis, Academic Press, New York, 1983.*

[5] Kalyanasundaram, K. Photophysics, photochemistry and solar energy conversion with tris(bipyridyl)ruthenium(II) and its analogues. *Coord. Chem. Rev.*, *46*, 159-244, 1982.

[6] Kalyanasundaram, K.; Grätzel, M. *Photosensitization and Photocatalysis Using Inorganic and Organometallic Compounds, Kluwer Academic Publishers, Dordrecht, 1993.*

[7] Sacksteder, L.; Lee, M.; Demas, J. N.; DeGraff, B. A. Long-lived, highly luminescent rhenium(I) complexes as molecular probes: intra- and intermolecular excited-state interactions. *J. Am. Chem. Soc.*, *115*, 8230-8238, 1993.

[8] Yam, V. W.-W.; Wong, K. M.-C.; Lee, V. W.-M.; Lo, K. K.-W.; Cheung, K.-K. Synthesis, photophysics, ion-binding studies, and structural characterization of organometallic rhenium(I) crown complexes. *Organometallics*, *14*, 4034-4036, 1995.

[9] Yoon, D. I.; Berg-Brennan, C. A.; Lu, H.; Hupp, J. T. Synthesis and preliminary photophysical studies of intramolecular electron transfer in crown-linked donor- (chromophore-) acceptor complexes. *Inorg. Chem.*, *31*, 3192-3194, 1992.

[10] Calabrese, J. C.; Tam, W. Organometallics for non-linear optics: Metal-pyridine and bipyridine complexes. *Chem. Phys. Lett.*, *133*, 244-245, 1987.

[11] Ehler, T. T.; Malmberg, N.; Carron, K.; Sullivan, B. P.; Noe, L. J. Studies of Organometallic Self-Assembled Monolayers on Ag and Au Using Surface Plasmon Spectroscopy. *J. Phys. Chem. B*, *101*, 3174-3180, 1997.

[12] Yam, V. W.-W.; Lau, V. C.-Y.; Cheung, K.-K. Synthesis, photophysics and photochemistry of novel luminescent rhenium(I) photoswitchable materials. *J. Chem. Soc. Chem. Com.*, 259-261, 1995.

[13]    Connick, W. B.; Di Bilio, A. J.; Hill, M. G.; Winkler, J. R.; Gray, H. B. Tricarbonyl(1,10-phenanthroline) (imidazole) rhenium(I): a powerful photooxidant for investigations of electron tunneling in proteins. *Inorg. Chim. Acta*, *240*, 169-173, 1995.

[14]    Di Bilio, A. J.; Crane, B. R.; Wehbi, W. A.; Kiser, C. N.; Abu-Omar, M. M.; Carlos, R. M.; Richards, J. H.; Winkler, J. R.; Gray, H. B. Properties of Photogenerated Tryptophan and Tyrosyl Radicals in Structurally Characterized Proteins Containing Rhenium(I) Tricarbonyl Diimines. *J. Am. Chem. Soc.*, *123*, 3181-3182, 2001.

[15]    Miller, J. E.; Di Bilio, A. J.; Wehbi, W. A.; Green, M. T.; Museth, A. K.; Richards, J. R.; Winkler, J. R.; Gray, H. B. Electron tunneling in rhenium-modified Pseudomonas aeruginosa azurins. *Biochim. Biophys. Acta*, *1655*, 59-63, 2004.

[16]    Biver, T.; Secco, F.; Venturini, M. Mechanistic aspects of the interaction of intercalating metal complexes with nucleic acids. *Coord. Chem. Rev.*, *252*, 1163-1177, 2008.

[17]    Ruiz, G. T.; Juliarena, M. P.; Lezna, R. O.; Wolcan, E.; Feliz, M. R.; Ferraudi, G. Intercalation of fac-[(4,4′-bpy) ReI(CO) 3(dppz)]+, dppz = dipyridyl[3,2-a:2′3′-c] phenazine, in polynucleotides. on the UV-vis photophysics of the Re(i) intercalator and the redox reactions with pulse radiolysis-generated radicals. *Dalton Trans.*, 2020-2029, 2007.

[18]    Armaroli, N.; Accorsi, G.; Felder, D.; Nierengarten, J.-F. Photophysical Properties of the ReI and RuII Complexes of a New C60-Substituted Bipyridine Ligand. *Chem. Eur. J.*, *8*, 2314-2323, 2002.

[19]    Bracco, L. L. B.; Juliarena, M. P.; Ruiz, G. T.; Féliz, M. R.; Ferraudi, G. J.; Wolcan, E. Resonance energy transfer in the solution phase photophysics of -Re(CO)3L+ pendants bonded to poly(4-vinylpyridine). *Journal of Physical Chemistry B*, *112*, 11506-11516, 2008.

[20]    Baxter, S. M.; Jones, W. E.; Danielson, E.; Worl, L.; Strouse, G.; Younathan, J.; Meyer, T. J. Photoinduced electron and energy transfer in soluble polymers. *Coord. Chem. Rev.*, *111*, 47-71, 1991.

[21]    Chen, L. X.; Jäger, W. J. H.; Gosztola, D. J.; Niemczyk, M. P.; Wasielewski, M. R. Ionochromic Effects and Structures of Metalated Poly(p-phenylenevinylene) Polymers Incorporating 2,2'-Bipyridines. *J. Phys. Chem. B*, *104*, 1950-1960, 2000.

[22]    Wang, B.; Wasielewski, M. R. Design and Synthesis of Metal Ion-Recognition-Induced Conjugated Polymers: An Approach to Metal Ion Sensory Materials. *J. Am. Chem. Soc.*, *119*, 12-21, 1997.

[23]    Wang, Q.; Wang, L.; Yu, L. Synthesis and Unusual Physical Behavior of a Photorefractive Polymer Containing Tris(bipyridyl)ruthenium(II) Complexes as a Photosensitizer and Exhibiting a Low Glass-Transition Temperature. *J. Am. Chem. Soc.*, *120*, 12860-12868, 1998.

[24]    Olmsted, J.; McClanahan, S. F.; Danielson, E.; Younathan, J. N.; Meyer, T. J. Electron and energy shuttling between redox sites on soluble polymers. *J. Am. Chem. Soc.*, *109*, 3297-3301, 1987.

[25]    Younathan, J. N.; McClanahan, S. F.; Meyer, T. J. Synthesis and characterization of soluble polymers containing electron- and energy-transfer reagents. *Macromol.*, *22*, 1048-1054, 1989.

[26]    Worl, L. A.; Strouse, G. F.; Younathan, J. N.; Baxter, S. M.; Meyer, T. J. Production and storage of multiple, photochemical redox equivalents on a soluble polymer. *J. Am. Chem. Soc.*, *112*, 7571-7578, 1990.

[27]    Jones, W. E.; Baxter, S. M.; Strouse, G. F.; Meyer, T. J. Intrastrand electron and energy transfer between polypyridyl complexes on a soluble polymer. *J. Am. Chem. Soc.*, *115*, 7363-7373, 1993.

[28]    Dupray, L. M.; Meyer, T. J. Synthesis and Characterization of Amide-Derivatized, Polypyridyl-Based Metallopolymers. *Inorg. Chem.*, *35*, 6299-6307, 1996.

[29]    Suzuki, M.; Kimura, M.; Hanabusa, K.; Shirai, H. Photosensitized charge separation using water-insoluble polymer-bound ruthenium(ii) complex films. *Journal of the Chemical Society, Faraday Transactions*, *93*, 4137-4143, 1997.

[30] Dupray, L. M.; Devenney, M.; Striplin, D. R.; Meyer, T. J. An Antenna Polymer for Visible Energy Transfer. *J. Am. Chem. Soc.*, *119*, 10243-10244, 1997.

[31] Friesen, D. A.; Kajita, T.; Danielson, E.; Meyer, T. J. Preparation and Photophysical Properties of Amide-Linked, Polypyridylruthenium-Derivatized Polystyrene. *Inorg. Chem.*, *37*, 2756-2762, 1998.

[32] Worl, L. A.; Jones, W. E.; Strouse, G. F.; Younathan, J. N.; Danielson, E.; Maxwell, K. A.; Sykora, M.; Meyer, T. J. Multiphoton, Multielectron Transfer Photochemistry in a Soluble Polymer. *Inorg. Chem.*, *38*, 2705-2708, 1999.

[33] Smith, G. D.; Maxwell, K. A.; DeSimone, J. M.; Meyer, T. J.; Palmer, R. A. Step-Scan FTIR Time-Resolved Spectroscopy Study of Excited-State Dipole Orientation in Soluble Metallopolymers. *Inorg. Chem.*, *39*, 893-898, 2000.

[34] Connors, P. J.; Tzalis, D.; Dunnick, A. L.; Tor, Y. Coordination Compounds as Building Blocks: Single-Step Synthesis of Heteronuclear Multimetallic Complexes Containing RuII and OsII. *Inorg. Chem.*, *37*, 1121-1123, 1998.

[35] Hou, S.; Chan, W. K. Polymer aggregates formed by polystyrene-block-poly(4-vinyl-pyridine) functionalized with rhenium(I) 2,2′-bipyridyl complexes. *Macrom. Rap. Com.*, *20*, 440-443, 1999.

[36] Bracco, L. L. B.; Einschlag, F. S. G.; Wolcan, E.; Ferraudi, G. J. On the mechanism of the photoinduced reduction of an adduct of ferricytochrome C with a poly(4-vinylpyridine) polymer containing -ReI (CO)3(3,4,7,8-tetramethyl-1,10-phenanthroline) pendants. *J. Photochem. Photobiol. A*, *208*, 50-58, 2009.

[37] Bracco, L. L. B.; Féliz, M. R.; Wolcan, E. On the quenching of MLCT luminescence by amines: The effect of nanoaggregation in the decrease of the reorganization energy. *J. Photochem. Photobiol. A*, *210*, 23-30, 2010.

[38] Bracco, L. L. B.; Lezna, R. O.; Muñoz-Zuñiga, J.; Ruiz, G. T.; Féliz, M. R.; Ferraudi, G. J.; Einschlag, F. S. G.; Wolcan, E. On the mechanism of formation and spectral properties of radical anions generated by the reduction of –[Re I(CO) 3(5-nitro-1,10-phenanthroline)] + and –[Re I(CO) 3(3,4,7,8-tetramethyl-1,10-phenanthroline)] + pendants in poly-4-vinylpyridine polymers. *Inorg. Chim. Acta*, *370*, 482-491, 2011.

[39] Wolcan, E.; Alessandrini, J. L.; Féliz, M. R. On the quenching of MLCTRe-bpy luminescence by Cu(II) species in Re(I) polymer micelles. *J. Phys. Chem. B*, *109*, 22890-22898, 2005.

[40] Wolcan, E.; Féliz, M. R. Temperature and medium effects on the photophysical properties of -Re(CO)3(2,2′-bipyridine) pendant chromophores coordinated to a poly(4-vinylpyridine) backbone. *Photochem. & Photobiol. Sci.*, *2*, 412-417, 2003.

[41] Wolcan, E.; Feliz, M. R.; Alessandrini, J. L.; Ferraudi, G. Aggregation in nanobundles and the effect of diverse environments on the solution-phase photochemistry and photophysics of -Re(CO)3L + (L = 1,10-phenanthroline, 2,2′-bipyridine) pendants bonded to poly(4-vinylpyridine). *Inorg. Chem.*, *45*, 6666-6677, 2006.

[42] Wolcan, E.; Ferraudi, G. Photochemical and photophysical properties of Fac-Re(I) tricarbonyl complexes: A comparison of monomer and polymer species with - ReI(CO)3phen chromophores. *J. Phys. Chem. A*, *104*, 9285-9286, 2000.

[43] Wolcan, E.; Ferraudi, G.; Feliz, M. R.; Gómez, R. V.; Mikelsons, L. UV photolysis of a Re(I) macromolecule, [(4-vinylpyridine)2 (4-vinylpyridineRe(CO)3(1,10-phenanthroline)+] 200: Addition of C-centered radicals to coordinated CO. *Supramolecular Chemistry*, *15*, 143-148, 2003.

[44] Féliz, M. R.; Ferraudi, G. Contrasting Intrastrand Photoinduced Processes in Macromolecules Containing Pendant -Re(CO)3(1,10-phenanthroline)+: Electron versus Energy Transfer. *Inorg. Chem.*, *43* 1551-1557, 2004.

[45] Moncada, A. S.; Einschlag, F. S. G.; Prieto, E. D.; Ruiz, G. T.; Lappin, A. G.; Ferraudi, G. J.; Wolcan, E. Photophysical properties of Re(I)(CO)3(phen) pendants grafted to a poly-4-vinylpyridine backbone. A correlation between photophysical properties and morphological changes of the backbone. *J. Photochem. Photobiol. A*, *321*, 284-296, 2016.

[46] Moncada, A. S.; Gutiérrez-Pineda, E.; Maisuls, I.; Ruiz, G. T.; Lappin, A. G.; Ferraudi, G. J.; Wolcan, E. Photochemical properties of a Re(I) polymer containing dppz in its structure. An interplay between dark and bright states of dppz. *J. Photochem. Photobiol. A*, *353*, 86-100, 2018.

[47] Cheng, K. W.; Chan, W. K. Morphology of Rhenium Complex-Containing Polystyrene-block-poly(4-vinylpyridine) and Its Use as Self-Assembly Templates for Nanoparticles. *Langmuir*, *21*, 5247-5250, 2005.

[48] Hou, S.; Man, K. Y. K.; Chan, W. K. Nanosized Micelles Formed by the Self-assembly of Amphiphilic Block Copolymers with Luminescent Rhenium Complexes. *Langmuir*, *19*, 2485-2490, 2003.

[49] Kumbhakar, M.; Nath, S.; Mukherjee, T.; Pal, H. Intermolecular electron transfer between coumarin dyes and aromatic amines in Triton-X-100 micellar solutions: evidence for Marcus inverted region. *J. Chem. Phys.*, *120*, 2824-2834, 2004.

[50] Rehm, D.; Weller, A. Kinetics of Fluorescence Quenching by Electron and H-Atom Transfer. *Isr. J. Chem.*, *8*, 259-271, 1970.

## Bio

### Ezequiel Wolcan

Ezequiel Wolcan obtained his BSc (1991) and Ph.D. (1996) at The National University of La Plata (UNLP), Argentina, after which he was the recipient of a Fulbright Research Scholarship at the University of Notre Dame, Indiana, USA. He returned to Argentina, where he joined the staff of the Institute of Research in Applied and Theoretical Physical Chemistry (INIFTA). He was appointed as a Full Professor at the UNLP in 2016. He is now a Principal Researcher of the Argentinian National Research Council (CONICET) at INIFTA where he leads a research group working on the photochemistry of coordination compounds in supramolecular structures, polymers and nanocomposites.